REPUBLIC OF TURKEY
YILDIZ TECHNICAL UNIVERSITY
GRADUATE SCHOOL OF NATURAL AND APPLIED SCIENCES

THE ANALYSIS OF THE NUCLEAR LOCALIZATION SIGNAL OF HEPATOCYTE NUCLEAR FACTOR-1α TRANSCRIPTION FACTOR

FAREED MOHAMMED ALI FAREED FAREED

MSc. THESIS
DEPARTMENT OF CHEMISTRY
PROGRAM OF GENERAL CHEMISTRY

ADVISOR
PROF. DR. BARBAROS NALBANTOĞLU

CO-ADVISOR
ASSIST. PROF. DR. ÖZLEM YALÇIN ÇAPAN

İSTANBUL, 2018

This study was supported by Scientific and Technological Research Council of Turkey (TUBITAK) Grant number: 116Z564.

ACKNOWLEDGEMENTS

I would like to thank my supervisor prof. Dr. Barbaros NALBANTOĞLU for his pure-hearted support and guidance throughout my study, also for giving me the opportunity to work on this project.

I would like to thank my Co-advisor Dr. Özlem YALÇIN ÇAPAN for introducing the molecular biology field to me, guiding me, teaching me with patience and dedication towards learning and mastering each technique and enriching my mind with the necessary information that made me interested more and more about this field.

I would like to thank TÜBİTAK for funding this project, and I also would like to thank Arel University for giving me the opportunity to work in their labs and for supporting this project with the necessary equipment.

I would thank my friends and specially Ihsan ALALLAK and Danial NICHOLA for supporting and lifting my spirit whenever needed, thank you for being my true friends.

Ultimately I would like to thank my mother, father, brother, and my sister for always believing in me, supporting me and love me the way I am, especially my father to whom I dedicate all of my work and this master degree.

December, 2018

Fareed FAREED

TABLE OF CONTENTS

Page

LIST OF SYMBOLS ……viii

LIST OF ABBREVIATIONS ……..ix

LIST OF FIGURES ……..... xi

LIST OF TABLES …… xii

ABSTRACT ……....xiii

ÖZET ……xv

CHAPTER 1

INTRODUCTION.....1

1.1 Literature Review…….....1
1.2 Aim of the Study…….....2
1.3 Hypothesis…….....2

CHAPTER 2

GENERAL INFORMATION ……4

2.1 Maturity Onset Diabetes of the Young (MODY)…….....4
2.1.1 Pathophysiology of MODY ……..... 4
2.1.2 Gene Mutations Related to MODY…….....….....6
2.1.3 HNF1A-MODY3…….....7
2.2 Nuclear Transport Mechanism…….....9
2.2.1 Nuclear Protein Transport Factors…….....10
2.2.2 The Classic Nuclear Protein Import Cycle…….....10
2.2.3 Karyophrines: Importin and Exportin……..... 13
2.2.4 Importin-α Transport Proteins...…….....13
2.2.5 Nuclear Localization Signal (NLS)…….....15
2.2.5.1 Classical Nuclear Localization Signal…….....15
2.2.5.2 The Importin α/cNLS Interaction……..…….....17

2.2.5.3 Non-classical Nuclear Localization Signal…….....18

CHAPTER 3

MATERIALS AND METHODS …….20

3.1 Materials …….....20
3.1.1 Equipments …….....20
3.1.2 Cell Line ……..…….....21
3.1.3 Chemical Materials and Antibodies…….....21
3,1.4 Primers …….....22
3,1.5 Used Strains ……..…….....23
3.1.6 Liquid and Solid Media ……..…….....23
3.1.7 Vectors …….....24
3.1.8 Kits Used in This Study …….…….....25
3.1.9 Buffers and Solutions……..…….....25
3.2 Methods 25
3.2.1 Mutant Plasmid construction by in vitro mutagenesis…….....25
3.2.2 Plasmid isolation …….....27
3.2.3 Cell culture studies …….....28
3.2.4 Co-immunoprecipitation Study…….....29
3.2.4.1 Total Protein Extraction……..…….....29
3.2.4.2 Co-immunoprecipitationAssay…….....30
3.2.4.3 Western Blot Analysis ……..…….....31
3.2.5 siRNA Silencing and Immunolocalization Study …….....32
3.2.5.1 siRNA with Silencing …….....33
3.2.5.2 Immunocytochemical Staining Assay ……..... 34

CHAPTER 4

RESULTS ……..…..35

4.1 Verification of Mutant HNF1A and Kpna Expression Vectors …….....35
4.2 Co-immunoprecipitation Assay of Wild-type HNF1A and Kpna Proteins in COS-7 Cells ……..…….....37
4.3 Co-immunoprecipitation Assay with Kpna6 and Mutant HNF1A Proteins in COS-7 Cells……..…….....39
4.4 Downregulation of Mouse Kpna6 Transport Protein with siRNA and Immunolocalization Analysis of HNF1A Protein in MIN6 Cells……..…….....40
4.4.1 The Effect of Kpna-specific siRNA on the Localization of HNF1 Protein in MIN6 Cells …….....40
4.4.1.1 Effects of Kpna-specific siRNA on the Level of Kpna Protein in Min6 Cells……..…….....45
4.4.2 Effects of Control Negative siRNA Treatment on HNF1A and Kpna6 Protein Levels…….....…….....48

4.4.3 Analysis of Co-localization of HNF1A and Kpna6 Proteins by Using Immunocytochemical Staining…….....52

CHAPTER 5

RESULTS AND DISSCUSSION …..……..54

REFERENCES …….57

CURRICULUM VITAE ……..67

LIST OF SYMBOLS

°C	Degree Celsius
h	Hour
L	Liter
µ	Micro
α	Alpha
β	Beta
M	Molarity
P	Pico
U	Unified atomic mass unit
g	Gram
xg	Against gravity
V	Volt
n	Nano

LIST OF ABBREVIATIONS

ABCC8	ATP binding cassette subfamily C member 8
APS	Ammonium persulfate
AldoB	Aldolase B
APPL1	Adaptor protein, phosphotyrosine interacting with PH domain and leucine Zipper 1
ARM	Armadillo repeats
ATP	Adenosine triphosphate
BLK	Lymphoid tyrosine kinase
BSA	Bovine serum albumin
CAS	CRISPER associated endonuclease
Ca	Calcium
cDNA	Complimentary DNA
CMV	Cytomegalovirus
Cse 1	Chromosome segregation 1
DAPI	4′,6-diamidino-2-phenylindole
DMEM	Dulbecco's Modified Eagle's medium
DMSO	Dimethyl sulfoxide
DNA	Deoxyribonucleic acid
dNTP	Deoxyribonucleotide triphosphate
EDTA	Ethelenediaminetetraacitic acid
FBS	Fetal bovine serum
GCK	Glucokinase
Glut2	Glucose transporter 2
GTP	Guanosine triphosphate
HCl	Hydrogen chloride
HNF	Hepatocyte nuclear factor
HNF1A	Hepatocyte nuclear factor 1 alpha
IAPP	Islet amyloid poly-peptide
IB	Immunoblotting
IBB	Importin beta binding domain
Ins-1 and 2	Genes encoding insulin
IP	Immunoprecipitation
IPF-1	Insulin promoter factor 1
K	Potassium
K (amino acid)	Lysine

KCNJ11	Potassium voltage-gated channel subfamily J member 11
Kpna	Karyopherin
kDa	Kilodalton
LB	Lysogeny broth
LPK	Liver-specific - pyruvate kinase
LYS	Lysis buffer
MCS	Multiple cloning site
MES	2-ethanesulfonic acid
Myc	MYC proto-oncogene
NaCl	Sodium chloride
NaOH	Sodium hydroxide
Neuro-D1	Neurogenic differentiation factor 1 / β- cell E-box transactivator 2
NLS	Nuclear localization signal
NP	Nucleoplasmin
NPC	Nuclear pore complex
NUP	Nucleoporine
NTF2	Nuclear transport factor-2
PAGE	Poly acrylamide gel electrophoresis
PAX4	Paired box 4
PBS	Phosphate-buffered saline
PBST	Phosphate buffer silane/ tween
PCR	Polymerase chain reaction
PDX1	Pancreatic and duodenal homeobox 1
Pen/Strept	Penicillin/ Streptomycin
Ran-GAP	Ran GTPase activating protein
Ran GTPase	Guanine nucleotide-exchange factor
Ran-GTP	Related nuclear protein- guanosine triphosphate
RES	Resuspension buffer
RNA	Ribonucleic acid
SHP-1	Small heterodimer partner 1
SV40	The polyomavirus simian virus 40
siRNA	Silencing ribonucleic acid
TEMED	Tetramethylethyleneediamine
ZIC3	Zinc finger protein family 3

LIST OF FIGURES

Page

Figure 2.1 Glucose metabolism and insulin production……..….....5
Figure 2.2 Three-dimensional structure of HNF1A protein……..…….....8
Figure 2.3 Structure and functional regions of the HNF1A protein…….....9
Figure 2.4 The nuclear envelope (NE) and the nuclear pore complex (NPC).....9
Figure 2.5 The molecular import pathway mechanism……..….....12
Figure 2.6 Importin α major and minor NLS-binding surface……..…….....14
Figure 2.7 The classical nuclear import complex…….....….....15
Figure 2.8 A, The interaction between importin-α and the classical nuclear localization signal. B, The effect of the autoinhibitory region on the N-terminal importinα…….....17
Figure 3.1 Mapping of the pCMV-Tag 2 vector……..……24
Figure 3.2 Multiple cloning site and promoter regions of the pCMV-Tag 2 vector……24
Figure 4.1 Verification of R271W (**C**GG→**T**GG) mutation generated by *in vitro* mutagenesis by DNA sequencing method…….....35
Figure 4.2 Confirmation of Kpna expression vectors by DNA sequence analysis….....36
Figure 4.3 Results of the co-immunoprecipitation assay showing the interactions between wild-type HNF1A and Kpna 2,4 and 6 transport proteins…….....37
Figure 4.4 Results of the repeated co-immunoprecipitation assay…….....38
Figure 4.5 Expression levels of Kpna proteins in different tissues……..….....38
Figure 4.6 Co-immunoprecipitation results are showing the interactions between Kpna transport protein and wild and mutant HNF1A proteins……....……39
Figure 4.7 Nuclear Localization of wild-type HNF1A transcription factors with Kpna6 specific siRNA and control negative siRNA-treatments…….....40
Figure 4.8 Analysis of nuclear localization of Kpna6 transport protein in Kpna6-specific siRNA-treated, negative control siRNA-treated and non-treated Min6 cells…….....……46
Figure 4.9 Results immunocytochemical staining and confocal analysis in siRNA treated cells, control negative siRNA-treated and non-treated cells for A) HNF1A and B) Kpna6 proteins…….....51
Figure 4.10 Co-localization of Kpna6 transport protein and HNF1A proteins in the cytoplasm of Min6 cells……..….....53
Figure 5.1 Impaired nuclear localization of S345Y mutation which resides in the non-classical NLS region.....54

LIST OF TABLES

Page

Table 2.1 Summarized information about MODY gene mutations…….....6

Table 2.2 Alternative names of importin α isoforms…….....14

Table 2.3 Examples of different types of nuclear localization signals……...16

Table 3.1 Cell lines……21

Table 3.2 Primer pairs used for in vitro mutagenesis study……22

Table 3.3 Sequences of the primer pair used for plasmid construction…….....23

Table 3.4 The chemicals required for the synthesis reaction of the mutant sequence in "in vitro mutagenesis technique"……26

Table 3.5 PCR amplification conditions for the newly synthesized mutant DNA……26

Table 3.6 Transfection reaction conditions and steps……29

Table 3.7 Volumes needed for the protein samples to be loaded to the gel……31

Table 3.8 Volumes needed for preparing 12% and 4% SDS-PAGE…….....31

Table 3.9 siRNA transfection reaction conditions and steps…….....33

Table 4.1 Results obtained from the whole cell and the cell nucleus for HNF1A protein in non-treated cells …….....41

Table 4.2 Results obtained from the whole cell and the cell nucleus for HNF1A protein inside siRNA-treated cells……43

Table 4.3 Results obtained from the whole cell for Kpna6 protein in siRNA-treated and non-treated cells……46

Table 4.4 Results obtained from the whole cell and the cell nucleus in control negative siRNA-treated cells for HNF1A protein…….....48

Table 4.5 Results obtained from the whole cell in control negative siRNA-treated cells for Kpna6 protein……50

ABSTRACT

THE ANALYSIS OF THE NUCLEAR LOCALIZATION SIGNAL OF HEPATOCYTE NUCLEAR FACTOR 1-α TRANSCRIPTION FACTOR

Fareed Mohammed Ali Fareed FAREED

Department of Chemistry

MSc. Thesis

Adviser: Prof. Dr. Barbaros NALBANTOĞLU

Co-Advisor: Assist. Prof. Dr. Özlem YALÇIN ÇAPAN

Maturity-onset diabetes of the young (MODY) is a monogenic subtype of diabetes mellitus. MODY3 associated with HNF1A gene mutations is the most common form of MODY. HNF1A protein is a transcription factor which is expressed mainly in pancreas, liver and kidney. Functional characterization of HNF1A gene mutations revealed that they affect DNA binding, transactivation function and nuclear localization of HNF1A. In previous studies R271W and S345Y mutant HNF1A were found to be defective in nuclear localization, but molecular mechanisms of this transport defect was not clarified yet.

Importin-α receptor family are responsible for translocating proteins such as transcription factors (HNF1A) into the nucleus. Importin proteins recognize and bind to nuclear localization signal (NLS) motifs which are found on cargo proteins. Although classic NLS motifs are known to consist of basic amino acids, non-classical NLS motifs were also reported. Importin α proteins are categorized into three groups based on the identity of amino acid sequence and function. To date, no single import signal in the HNF1A protein has been identified, but there are three regions that fit the description of an NLS: region A (amino acids 158-171), region B (amino acids 197-205) and region C (amino acids 271-282). However, importin α subtype which recognizes and binds to HNF1A has not been reported yet.

One of the aims of this study is to identify the importin α subgroup which is responsible for the transport of HNF1A protein into the nucleus. For this purpose the interactions of HNF1A with three candidate importin α proteins were be evaluated by co-immunoprecipitation technique. In this study, homolog mouse karyopherin α proteins (Kpna2, 4 and 6) were used. The results of co-IP revealed that HNF1A protein is recognized and bound by all three importin α subgroup proteins. The strongest band was observed with Kpna6 protein, therefore in the following part of the experiment the interactions with Kpna6 protein were analyzed. To confirm this interaction, Kpna6 was knockdown by siRNA in mouse pancreatic cells (MIN6) and the location of HNF1A was analyzed by immunochemical staining techniques. The results showed that there is 10% reduction in the nuclear localization of HNF1A protein when the Kpna6 protein is silenced. Second purpose of the study was to analyze the interaction between predetermined importin α subgroup and mutant HNF1A proteins (R271W and S345Y) which were identified in MODY patients. R271W mutation resides in a region similar to classical NLS motif of HNF1A protein. Therefore, the interaction between mutant HNF1A and importin α will be evaluated by co-immunoprecipitation technique. A reduced interaction was observed when compared to the interaction with the wild type and this confirmed that R271W mutation resides in the classical NLS motif in HNF1A protein. S345Y mutation is on the other hand, does not reside in a classical NLS, but was shown to have nuclear localization defect in functional studies. A reduced interaction of S345Y mutant protein with Kpna6 protein was detected and this result showed that this region is a possible non-classical NLS motif in HNF1A protein.

As a conclusion, the results of this study clarified the molecular pathway of nuclear import of HNF1A protein and molecular pathogenesis of HNF1A mutations in MODY3 patients. Also the identification of non-classical NLS motifs in HNF1A protein will contribute to the literature and also will provide a preliminary result for further projects.

Keywords: Maturity-onset diabetes of the young, MODY, Diabetes, HNF1A, importin α, Kpna, Nuclear localization signal (NLS).

ÖZET

HEPATOCYTE NÜKLEAR FACTÖRÜ 1-α TRANSKRİPSİYON FAKTÖRÜNÜN NÜKLEAR LOKALİZASYON SİNYALİNİN ARAŞTIRILMASI

Fareed Mohammed Ali Fareed FAREED

Kimya Anabilim Dalı

Yüksek Lisans Tezi

Tez Danışmanı: Prof. Dr. Barbaros NALBANTOĞLU

Eş Danışman: Dr. Öğr. Üyesi Özlem YALÇIN ÇAPAN

MODY (Maturity onset of diabetes of youth) diyabetin tek gene bağlı bir alt grubu olup en sık görülen tipi MODY3'tür. MODY3 hastalarında pankreas, böbrek ve karaciğerde görevli transkripsiyon faktörü olan HNF1A geninde mutasyonlar tespit edilmiştir. Bu mutasyonlar proteinin DNA'ya bağlanmasını, transaktivasyon fonksiyonunu ya da hücre çekirdeğine lokalize olmasını etkilemektedirler. Önceki çalışmalarda mutant R271W ve S345Y HNF1A proteinlerinin hücre çekirdeğine lokalize olmalarının hasarlı olduğu tespit edilmiştir. Ancak bu hasarın moleküler mekanizması henüz aydınlatılmamıştır.

İmportin α taşıma reseptör ailesi transkripsiyon faktörü gibi hücre çekirdeğinde görevli proteinlerin hücre çekirdeğine taşınmasından sorumludur. Bu proteinler kargo proteinlerine kargo proteinler üzerinde bulunan NLS (Nuclear localization signal) motifleri üzerinden bağlanmaktadır. Klasik NLS motifleri bazik amino asitler içermesine rağmen, klasik olmayan NLS motiflerinin de bulunduğu gösterilmiştir. İmportin α, amino asit ve fonksiyonel benzerlik olarak 3 alt gruba ayrılmaktadır. Şu ana kadar HNF1A proteini üzerinde belli bir import sinyal motifi rapor edilmemiş olsa da HNF1A proteini ile yapılan çalışmalarda klasik NLS bölgesi tanımına uyan 3 bölge (A, B ve C bölgeleri) olduğu gösterilmiştir. A bölgesi HNF1A proteininde 158-171 amino asitleri arası, B bölgesi 197-205 amino asitler arası ve C bölgesi 271-282 amino asitler

arasında yer almaktadır. Ancak HNF1A'nın taşınmasından sorumlu importin α alt grubu ve diğer klasik olmayan NLS bölgeleri henüz rapor edilmemiştir.

Yürütülen bu projenin ilk amacı, HNF1A transkripsiyon faktörünün hücre çekirdeğine taşınmasından sorumlu importin α alt grubunun tespit edilmesidir. Bu amaçla importin α proteinin 3 farklı alt grubu fare homolog karyopherin α proteinlerinden (Kpna2, 4 ve 6) seçilmiş ve seçilen proteinlerle HNF1A arasındaki etkileşim ko-immunoçöktüme yöntemiyle araştırılmıştır. Bu çalışma ile yabanıl HNF1A proteinin her 3 taşıyıcı protein ile de etkileşim halinde olduğu görülmüştür. En güçlü bağlanmayı Kpna6 proteini ile gösterdiğinden, projenin sonraki aşamalarında Kpna6 proteini ile devam edilmiştir. Bu etkileşimi doğrulamak için fare pankreas hücrelerinde (Min6) tespit edilen Kpna6 proteini siRNA kullanılarak susturulma çalışması yapılmış ve immunositokimyasal boyama çalışmasıyla HNF1A proteinin hücre içindeki lokalizasyonu araştırılmıştır. Kpna6 proteinin susturulması ile HNF1A'nın hücre çekirdeğine %10 daha az lokalize olduğu tespit edilmiştir. Projenin ikinci amacı ise MODY hastalarında tespit edilen ve hücre çekirdeğine lokalizasyonu hasarlı mutant HNF1A proteinleri (R271W ve S345Y) ve importin α alt grubu arasındaki etkileşimin araştırılmasıdır.

R271W mutasyonu klasik NLS motifleri içerisinde olup, tespit edilen importin α alt grubunun HNF1A'yı tanıyıp bağlanma bölgesinde yer almaktadır. Bu sebeple R271W mutant HNF1Ave Kpna6 taşıyıcı protein arasındaki etkileşim ko-immunoçöktürme yöntemiyle araştırılmıştır. Yabanıl tip HNF1A ile karşılaştırıldığında R271W mutant HNF1A proteini ile Kpna6 proteini arasında daha az etkileşim olduğu görülmüştür. Bu sonuç R271W mutasyonunun proteinin klasik bir NLS motifi içerisinde yer aldığını doğrulamış oldu. S345Y mutant HNF1A proteini ise klasik bir NLS motifi içerisinde bulunmamasına rağmen, hücre çekirdeği lokalizasyonunda hasarlı olduğu tespit edilmiştir. Ko-immunoçöktürme çalışmalarında, bu mutant HNF1A proteinin, Kpna6 taşıyıcı protein ile etkileşiminde azalma gözlemlenmiş, bu da bu bölgenin klasik olmayan bir NLS bölgesi olduğunu desteklemektedir.

Sonuç olarak yürütülen bu proje ile ilk defa HNF1A transkripsiyon faktörünün hücre çekirdeğine taşınma yolağında görevli taşıyıcı proteinler tespit edilmiş ve MODY3 hastalarında hastalığa sebep olan mutasyonların moleküler patogenezinin aydınlatılmasına katkı sağlamıştır. Ayrıca S345Y mutasyonun HNF1A proteinin üzerinde klasik olmayan NLS bölgesinde bulunduğu hipotezi de desteklenmiştir. Bu çalışmanın sonuçları, klasik olmayan NLS bölgeleri ile ilgili literatüre katkı sağlamış olacak ve daha detaylı projelerin hazırlanmasına önveri oluşturacaktır.

Anahtar Kelimeler: Maturity-onset Diabetes of the Young, MODY, Diyabet, HNF1A, Importin α, Kpna, Nüklear lokalizasyon sinyali (NLS)

CHAPTER 1

INTRODUCTION

1.1 Literature Review

Maturity Onset Diabetes of the Young (MODY) is an autosomal dominant inherited disease diagnosed by asymptomatic hyperglycemia in non-obese young patients caused by the loss in function of pancreatic beta-cells [1], [2], [3]. Recent studies have successfully identified 14 MODY genes and their related heterozygous mutations [4], [5], [6]. Glucokinase gene mutations (MODY2), transcription factor HNF1A (MODY3) and HNF4A (MODY1) gene mutations are the most common types of MODY [7].

MODY3 is a disease found to be associated with mutations in the HNF1A gene. HNF1A, a homeodomain transcription factor, is expressed in different tissues such as pancreas, liver, and kidney. Besides liver-specific genes, HNF1A plays a role in glucose metabolism (e.g., pyruvate kinase), glucose transport (e.g., GLUT2) and insulin gene expression [8]. The HNF1A molecule, consists of three functional regions: the N-terminal dimerization, the pseudo-POU and the DNA binding region containing the Homeodomain motif, and the C-terminal transactivation site [9]. Among the reported mutations (R271W) [1] and (S345Y) were found to be defective in nuclear localization, but the molecular transport was not clarified.

Proteins that are destined to be transported to the nucleus contain amino acid sequences called the Nuclear Localization Signal (NLS). In each protein, the best-identified signal is called classical NLS. Classical Nuclear localization signal is assorted into either (monopartite) or (bipartite), this cNLS is recognized by the transporter proteins to be translocated into the nucleus [10], [11], [12]. Some molecular components required for the nuclear transport of proteins have been identified [13], [14].

The nuclear pore complex (NPC) are pores located on the surface of the nucleus, these pores were found selective. For some molecules such as transcription factors cannot pass this pore. In fact, these processes are actively carried out by the importin systems. Importin has two subunits; importin α and importin β, cargo proteins which contain the classical NLS are bound by importin α, importin α is an adapter between the cargo proteins and importin β [15]. The cargo protein- importin α- importin β heterotrimeric complex formed in the cytoplasm is recognized by the nuclear pore complex settle in the nucleus [15]. Importin α is assorted into three groups according to their amino acid sequence. The first group includes the human importin α and mouse karyopherin α2 (Kpna 2); the second group comprised of human importin α3 and α4, their correspondent mouse proteins are Kpna3 and Kpna4 respectively; the last group contains human importin α5, α6 and α7 and mouse Kpna1 and Kpna 6 [16].

To date, no single import signal in the HNF1A protein has been identified, but three regions fit the description of an NLS: region A (amino acids 158-171), region B (amino acids 197-205) and region C (amino acids 271-282). However, importin α subtype which recognizes and binds to HNF1A has not been reported yet [1].

1.2 Aim of The Study

This study will clarify the molecular pathway of nuclear import of HNF1A protein and molecular pathogenesis of HNF1A mutations in MODY3 patients. Also, identification of non-classical NLS motifs in HNF1A protein will contribute to the literature.

1.3 Hypothesis

One of the purposes of the proposed study is to identify the importin α subgroup which is responsible for the transport of HNF1A protein into the nucleus. For this purpose, the interaction of HNF1A with three candidate importin α proteins will be evaluated by co-immunoprecipitation technique. Positive bands will indicate the specific importin α subgroup which recognizes and binds to HNF1A. To confirm this interaction, specific importin α protein will be knockdown by siRNA in mouse pancreatic cells (MIN6), and immunochemical staining techniques will analyze the location of HNF1A. A defect in nuclear localization will confirm that specific importin α subgroup is responsible for HNF1A import. The second purpose of the study is to analyze the interaction between predetermined importin α subgroup and mutant HNF1A proteins (R271W and S345Y) which were determined in MODY patients. R271W mutation resides in a region similar

to classical NLS motif of HNF1A protein. Therefore, the interaction between mutant HNF1A and importin α will be evaluated by co-immunoprecipitation technique. A reduced interaction compared to the interaction with the wild-type will confirm the classical NLS motif in HNF1A protein. S345Y mutation, on the other hand, does not reside in a classical NLS but was shown to have nuclear localization defect in functional studies. A reduced interaction of the S345Y mutant protein with importin α will indicate that this region is a possible non-classical NLS motif in HNF1A protein.

CHAPTER 2

GENERAL INFORMATION

2.1 Maturity Onset Diabetes of The Young (MODY)

Maturity Onset Diabetes of the Young (MODY) is an autosomal dominant inherited disease diagnosed by asymptomatic hyperglycemia in non-obese young patients caused by the loss in function of pancreatic beta-cell [1], [2], [3]. MODY has a high possibility to be inherited and exhibiting a continuous type monogenic forms of diabetes which are related to the newborn infants [17], [18], [19]. Seven of the functional MODY genes encode for transcription factors which are involved in the β-cell development, maturation, and maintenance. The other MODY types are mainly related to the insulin secretion process depending on the glucose level in the body [17], [18], [19]. Recent studies have successfully identified 14 MODY genes and their related heterozygous mutations, and there are more to be discovered in the future [17], [20]. The consideration of MODY disease as either type 1 or type 2 diabetes is frequently a common mistake [21]. Accordingly, patients with monogenic diseases like MODY should be diagnosed using molecular genetics in order to obtain an accurate diagnosis, and this will ultimately impact the patient's treatment [21].

2.1.1 Pathophysiology of MODY

MODY is generally symptomized by the impairment of insulin secretion as a result of the ß-cell dysfunction; this impairment is caused by certain mutations in the glycolytic enzyme glucokinase and five nuclear transcription factors [22]. Glucose obtained from the bloodstream by glucose transporters (GLUT 2) passes through the cell membrane of the pancreatic ß-cells [22]. The glucose than gets converted into glucose-6-phosphate by the aid of the intracellular enzyme Glucokinase, this step is considered the initiation step of glucose metabolism. The glucose-6-phosphate then enters the mitochondria and

undergo glycolysis and then enters Krebs cycle to produce adenosine triphosphate ATP. This ATP will be consumed to provide energy for potassium ion to be pumped out of the cell membrane through ATP dependent potassium channels [22]. This pumped out potassium will allow the calcium ions to be pulled into the ß-cell. This ion circulation as demonstrated in Figure 2.1 will provide enough energy for the formed insulin to be released out of the cell [22]. Hepatic Nuclear Factors and nuclear transcription factors are essential for the synthesis of insulin inside ß cells [22].

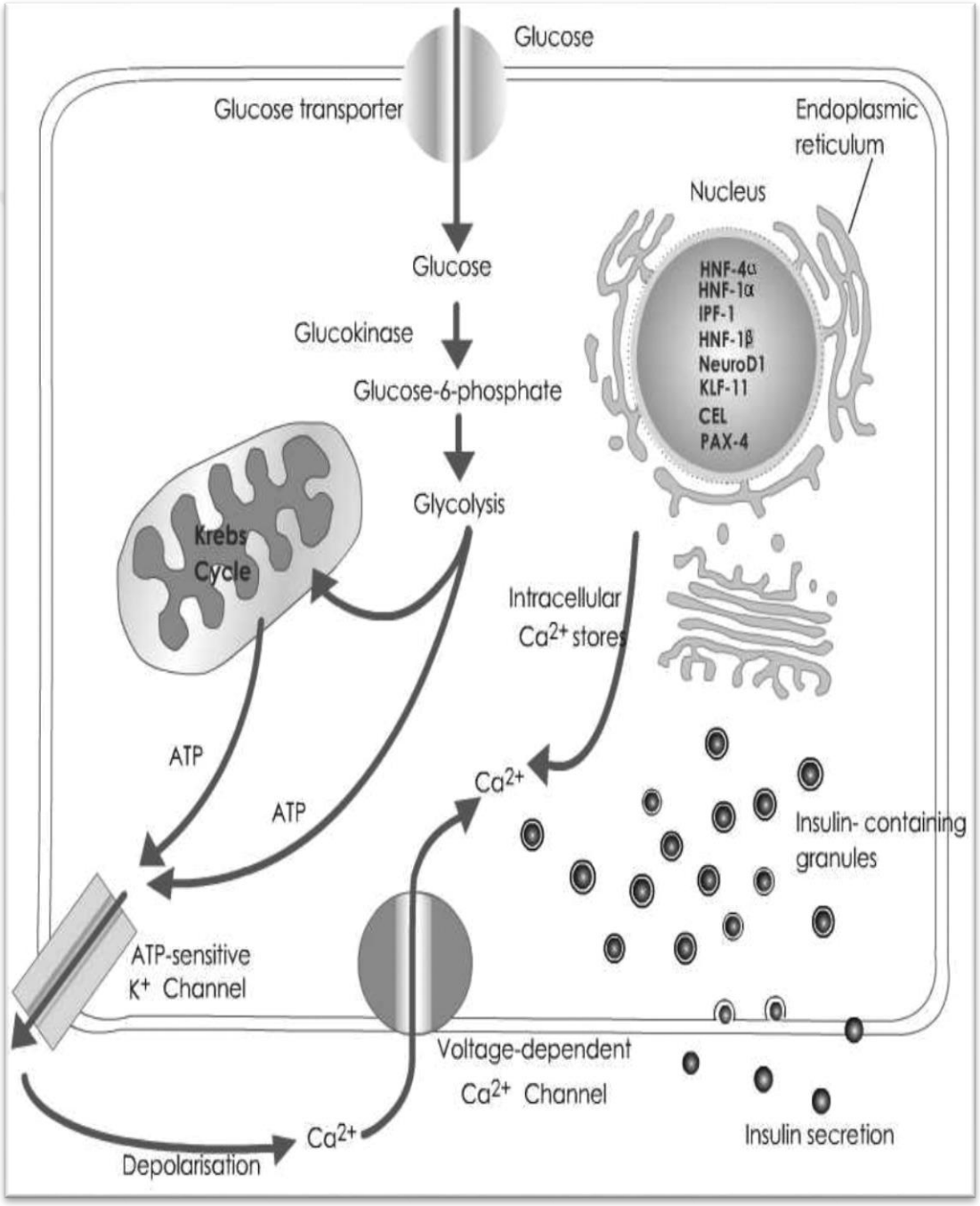


Figure 2.1 Glucose metabolism and insulin production [23].

2.1.2 Gene Mutations Related To MODY

Until the present day, 14 type of gene mutations were found pertaining to MODY disease [6],[7]. Table 2.1 summarizes each gene, the encoded protein and the percentage of occurrence in patients. Among all MODY types, glucokinase gene mutations (MODY2), transcription factor HNF1A (MODY3) and HNF4A (MODY1) gene mutations were found to have the highest percentage in the occurrence of any other MODY type [6],[7]. It is debatable which MODY is the most common, in some reports MODY 2- GCK is the most common but in other reports MODY3-HNF1A is the most common, This discrepancy may in part be explained by different ways of patient selection [5], [6].

Table 2.1. Summarized information about MODY gene mutations.

Gene (Locus Name)	**% of All MODY**	**Clinical Features**	**Encoded Protein**	**References**
ABCC8 (MODY12)	<1%	Similar to HNF1A- & HNF4A-MODY	SUR1	[5]
APPL1 (MODY14)	<1%	Overweight/obesity in some	Adaptor Protein, Phosphotyrosine Interacting With PH Domain And Leucine Zipper 1	[20]
BLK (MODY11)	<1%	Overweight/obesity in some	Tyrosine-protein kinase BLK	[24],[25]
CEL (MODY8)	<1%	Pancreatic atrophy → exocrine pancreatic insufficiency Fibrosis & lipomatosis → diabetes	Bile salt-activated lipase	[26],[27]
GCK (MODY2)	30%-50%	Stable, mild fasting hyperglycemia at birth Typically asymptomatic; diagnosis often incidental	Glucokinase	[28],[29]
HNF1A (MODY3)	30%-65%	Transient neonatal hyperinsulinemic hypoglycemia in some Progressive insulin secretory defect OGTT frequently needed to make an early diagnosis Renal glycosuria	Hepatocyte Nuclear Factor 1 Alpha	[30]

Table 2.1. Summarized information about MODY gene mutations. (Continued)

HNF1B (MODY5)	<5%	IUGR Renal anomalies Urogenital tract anomalies Pancreatic hypoplasia	Hepatocyte Nuclear Factor 1 Beta	[31], [32], [33], [34]
HNF4A (MODY1)	5%-10%	Birth weight >800 g above normal Transient neonatal hyperinsulinemic hypoglycemia common Progressive insulin secretory defect	Hepatocyte Nuclear Factor 4 Alpha	[22],[35], [36], [37]
INS (MODY10)	<1%		Insulin	[38],[39]
KCNJ11 (MODY13)	<1%	Similar to HNF1A-MODY & HNF4A-MODY	KIR6.2	[7],[40]
KLF11 (MODY7)	<1%		Krueppel-like factor 11	[41],[42]
NEUROD1 (MODY6)	<1%	Overweight/obesity in some	Neurogenic differentiation factor 1	[43],[44]
PAX4 (MODY9)	<1%		Paired box factor Pax4	[45],[46]
PDX1 (MODY4)	1%	Overweight/obesity in some	Pancreas/ Duodenum homeobox protein 1	[47]

2.1.3 HNF1A-MODY3

HNF-1A is a transcription factor (Figure 2.2) by which various specific genes in the liver and pancreas are regulated. This gene is involved mainly in glucose transport and metabolism in addition to the amino acid and lipid metabolism [48]. Any alteration in HNF1A gene would cause a diabetic disease called “MODY3” which is considered to be the most common MODY type due to the high level of inheritance among the other MODY types [49]. MODY 3 is observed by the reduction in insulin secretion due to a pancreatic β-cell dysfunction before the age of 25 [49]. 300 different HNF1A gene mutations were identified in MODY3 patients; these mutations are listed in the human genome mutation database. The patient will be diagnosed mainly by determining the location of this mutation. Accordingly, patients with mutations in the terminal exons (8–

10) are diagnosed approximately eight years earlier than those with mutations in exons (1–6) [50].

HNF1α is expressed in liver, kidney, intestine and pancreatic islets [51]. By now, >100 genes regarded as liver-specific are regulated potentially by HNF1α [52]. The human HNF1α gene is comprised of 10 exons encode for a transcription factor of 631 amino acids and composed of a short N-terminal dimerization domain (amino acids 1–32), a POU-homeobox DNA-binding domain (amino acids 150–280) and a C-terminal transactivation domain (amino acids 281–631) (Figure 2.3) [53],[54].

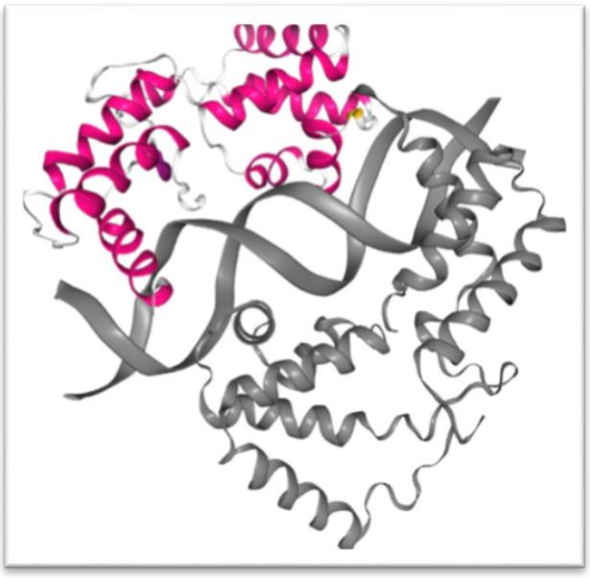


Figure 2.2 Three dimensional structure of the HNF1A protein.

The predetermined HNF1A gene mutations were comprised of a frameshift, missense, nonsense and splice site mutations [54], [55]. A high percentage of the mutations located in the DNA-binding domain or the transactivation domain of HNF1α, as shown in Figure 2.3, is supposed to function in a negative-dominant manner [56]. Other mutations in association with the MODY3 phenotype that has been identified in the promoter region [56] and dimerization domain [57] of HNF1α would result a reduced HNF1α gene dosage. MODY3 mutants that form proteins with reduced stability or decreased transactivation would also elicit haploinsufficiency [57].

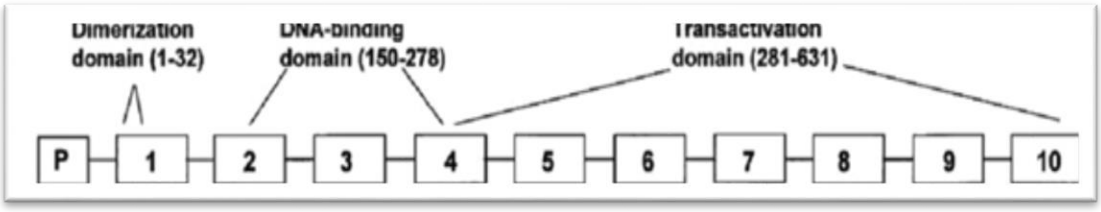


Figure 2.3 Structure and functional regions of the HNF1A gene (P: Promoter region) [9]

2.2 Nuclear Transport Mechanism

Molecular diffusion of macromolecules between the cytoplasm and the nucleoplasm is maintained by a physical barrier located on the surface of the nucleus called "the nuclear envelope", this envelope consists of a phospholipid bilayer membrane which on its turn comprised of an inner and outer membrane and they are separated by a perinuclear space [58], [59] as shown in Figure-2.4 a. The nuclear pore complex (NPC) is a pore 30 nm in diameter, allow the ions and small molecules such as proteins with a molecular mass up to 40kDa to be translocated from or to the nucleus [59].

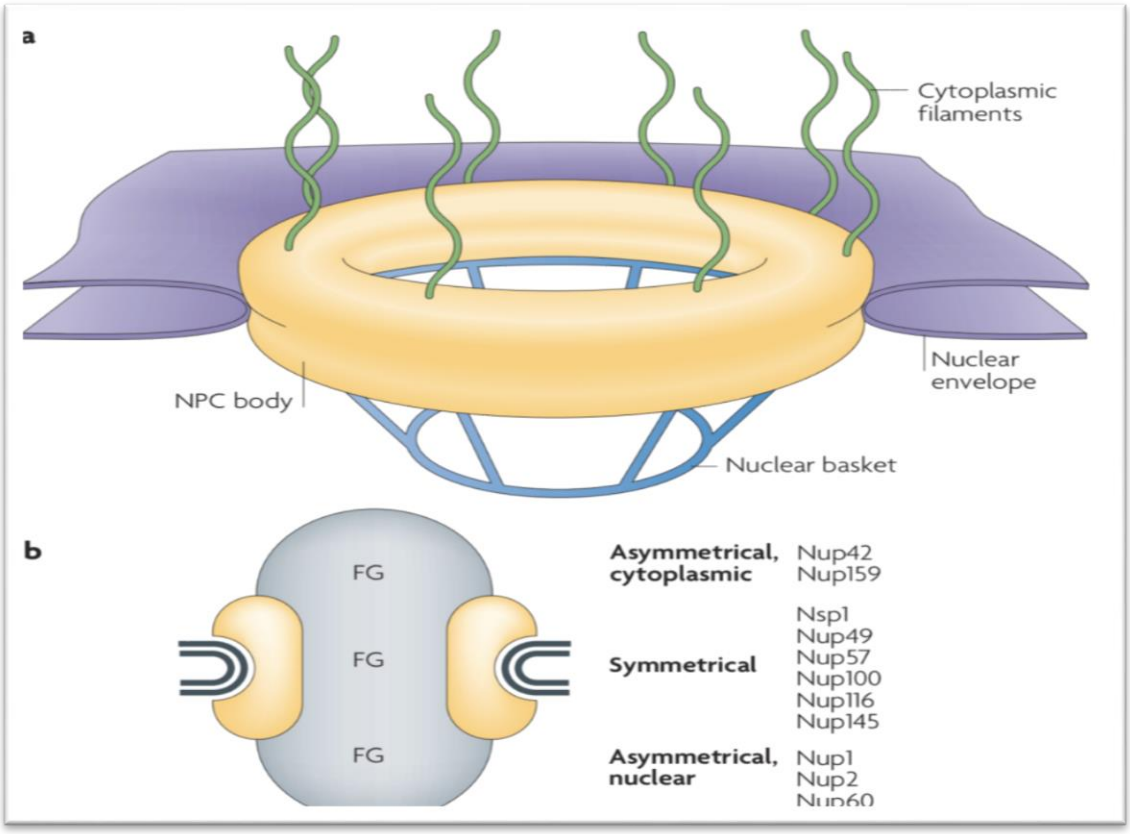


Figure 2.4 The nuclear envelope (NE) and the nuclear pore complex (NPC) [60]
a) Nuclear pore complex b) Nucleoporin types

Transporting larger molecules through the nuclear pore complex requires certain energy-dependent mechanisms [61]. The pores are constructed from a class of proteins called “nucleoporins”. Nucleoporins were generally aligned across the NPC in both sides, the cytoplasmic and the nuclear; however, a small portion of nucleoporins was found misaligned on one side of the NPC [61], [62], this misalignment is attributed to the place where the roots are attached to the NPC [63]. Biochemical fractionation of NPCs has shown that many nucleoporins associate with one another to form subcomplexes with a defined composition [61]. Nucleoporins seem to be constructed from a number of common protein folds, including coiled coils, WD propellers and α-helical solenoids93. These folded domains are thought to be located primarily in the annular body of NPCs. Furthermore, the structure of nucleoporins was found to contain a distinctive sequence of Phe-Gly (FG) motifs [61],[64],[65], these motifs were found scattered throughout the entrance of pore5 and the central transport channel [66] (Figure 2.5 b).

2.2.1 Nuclear Protein Transport Factors

The nuclear pore complex is considered a very selective channel, it allows only the small proteins (<40 kDa) but blocks the way for larger molecules [67],[68]. The molecules that are destined to be transported from the cytoplasm to the cell nucleus and vice versa are carried by a specific carrier proteins known as "karyopherins" [69], Karyopherins involved in the transfer of the macromolecules from the cytoplasm to the cell nucleus are called "importins" [70], and karyopherins responsible for the transportation from the nucleus to the cytoplasm are called "exportins" [71]. In the actual transport system, there is no importin and exportin; these terms were given to distinguish between their tasks. Ideally, the transport factor which imported the molecule from the cytoplasm to the nucleus, switch to export mode and carry a different protein [72],[73]. Importin ß is a superfamily implicate many transport proteins, collectively they are called "ß-karyopherins" [74]. Some proteins are transported by directly binding to the ß-karyopherins; however, in classical nuclear import, the interaction between the β-karyopherin and the cargo is mediated by the adaptor molecule importin α [74].

2.2.2 The Classic Nuclear Protein Import Cycle

Approximately 100-1000 cargo protein is transported per minute per nuclear pore complex through the classical import cycle [75], this cycle is administrated by a

consecutive protein: protein interactions. Importin-α binds to the cargo proteins that contain a classical NLS; this complex is then bound to importin-β through importin-α [76], [77], [78], [79], [80], [81], [82], [83], [84], [85]. These transport proteins are constructed of repeated motifs and share an extended structure [77]. After the formation of the trimeric complex (cNLS cargo protein- importin- α:β), importin-β paves the way for importin-α and the cargo protein to enter through the NPC to the nucleus [86]. After delivering the cargo, RanGTP bind and separate importin-β from the cargo, RanGTP-importin-β is then recycled to the cytoplasm to be ready for carrying another complex [86]. Importin-α is dissociated from the cargo protein by the aid of RanGTP and β-karyopherin CAS [86]. The termination step for this process is carried out by the cytoplasmic RanGAP (Ran GTPase activating protein) stimulates the Ran GTPase, generating RanGDP, which dissociates from the importins and thereby releases them for another import cycle [86]. The import cycle is a sophisticated series of step by step interactions. Therefore the cycle should be administrated by a certain criteria [86]. The molecular recognition between each factor in the cycle and between transport proteins to the cargo protein is the main criteria. Ran is the main factor of regulation for this cycle, Ran cycles between GTP- and GDP- state (Figure 2.5) [86]. Cytoplasmic guanine-exchange factor (RanGEF) controls the Ran nucleotide state by stimulating the conversion of RanGDP to RanGTP in the cytoplasm. As a result, RanGAP hydrolyzes GTP in the nucleus and RanGEP recharge with GTP in the cytoplasm. This implies that nuclear Ran is in the GTP-bound state, whereas cytoplasmic Ran is GDP bound. RanGTP is exported from the nucleus bound to β-karyopherin carriers and, after RanGAP-mediated GTP hydrolysis, cytoplasmic RanGDP is transported to the nucleus by its specific carrier, nuclear transport factor-2 (NTF2) [87],[88], for recharging with GTP. The confirmation of key structural loops in Ran (the switch I and II loops) changes markedly with nucleotide state. This structural change determines the way in which importin-β family transport factors interact with cargoes, and so ultimately, the Ran GTPase provides the energy for nuclear transport. The nuclear protein import cycle can be conveniently divided into four steps: assembly of the cargo: carrier import complex in the cytoplasm; translocation through NPCs; import-complex disassembly in the nucleus; and importin recycling, (Figure 2.5) explain the cycle.

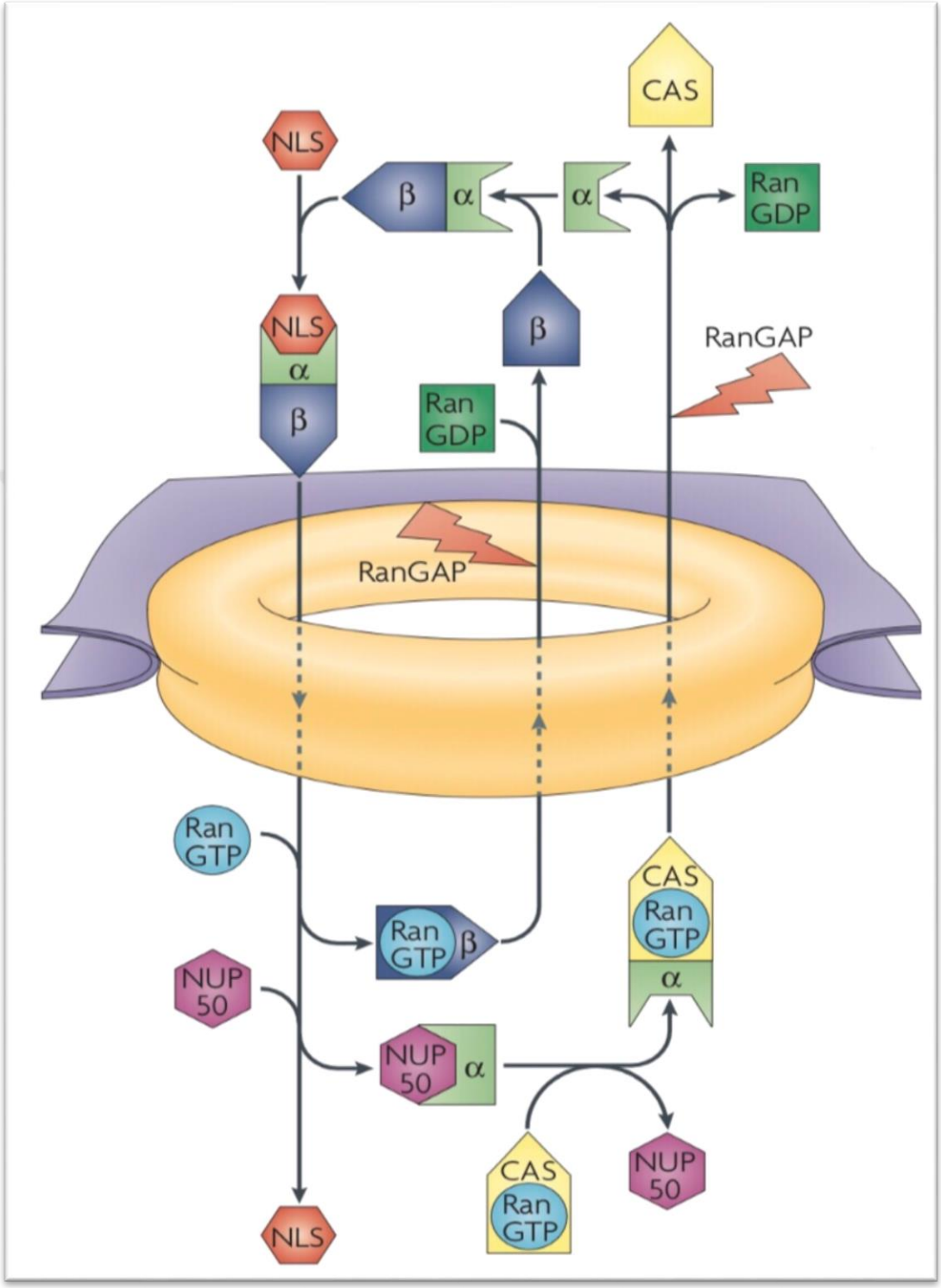


Figure 2.5 The molecular import pathway mechanism [86].

2.2.3 Karyophrines: Importin and Exportin

In the literature, more than 20 karyopherins were identified in human [89]. 11 of them were found responsible for importing the cargo protein from the cytoplasm to the nucleus or working bidirectionally, they are known as (importin-β, importin-β2, importin-4, importin-5, importin-7, importin-8, importin-9, importin-11, transportin-SR, importin-13, exportin-4) [89]. For the export mechanism, eight exportins (exportin-1–exportin-7, exportin-t) were implicated in the export of cargo molecules [89]. Each karyopherin has its specific cargo molecule [89]. For example, CAS (exportin-2) was found responsible for the export of importin-α, while exportin-t was found liable for the export of tRNA [90]. Karyopherins are also accountable for exporting some nucleotide motifs including tRNA, miRNA, rRNA, viral RNA, and uridine-rich small nuclear RNAs with or without ribonucleoprotein as an adaptor [90], [91], [92], [93], [94], [95].

2.2.4 Importin-α Transport Proteins

Importin-α isoforms were known to share the same basic structure which comprise of an N-terminal, autoinhibitory, IBB domain and C-terminal helical core. The N-terminal measures approximately the first 70 residues while the C-terminal core contains the Armadillo repeats (ARM-core) [96]. Importin-α isoforms share very high sequence similarity, but it also exhibits some slight differences in the 3D structure and biochemical properties, these variations gave each importin-α isoform *in vivo* the specificity for specialized import cargo [96]. A tandem series of Armadillo repeats (ARM) were identified in importin-α structure; these series contain an ordered arrangement of Trp, Asn and acidic residues in the inner surface [97], [98], [99]. Although ARM motif has three helical structures instead of two in HEAT motif, the superhelical 3D structure of ARM repeats is similar to that of HEAT repeats.

Importin-α family is assorted into three groups according to their amino acid sequence (Table 2.2) [16]. The first group includes the human importin-α and mouse karyopherin α2 (Kpna 2); the second group comprise of human importin-α3, and α4, their correspondent mouse proteins are Kpna 3 and Kpna 4 respectively; the last group contains human importin-α5, α6 and α7 and mouse Kpna 1 and Kpna6 as demonstrated in Table 2.2 [16]. The construction of the Arm-core of importin α1, α3, α5, and α7 reveals that the NLS-binding surface is practically identical in all the isoforms [96], only the NLS-binding sites are different between each isoform as shown in Figure 2.6 and 2.7. This explains that the binding affinity and the specificity of importin protein to

the cargo protein are not attributed to NLS-binding surface, for they were found identical [96].

Table 2.2 Alternative names of importin-α isoforms [96].

Subfamily	Protein names	Alternative names	Gene name
α1	Importin α1	Karyopherin α2, hSRP1α [100], Rch1 [101], Qip2 [102], NPI-3 [103].	KPNA2
	Importin α8	Karyopherin α7.	KPNA7
α2	Importin α3	Karyopherin α4, Qip1 [101].	KPNA4
	Importin α4	Karyopherin α3, hSRP1γ [104], Qip2 [105].	KPNA3
α3	Importin α5	Karyopherin α1, NPI-1 [106], SRP1 [107], hSRP1 [101].	KPNA1
	Importin α6	Karyopherin α5	KPNA5
	Importin α7	Karyopherin α6, NPI-2 [108]	KPNA6

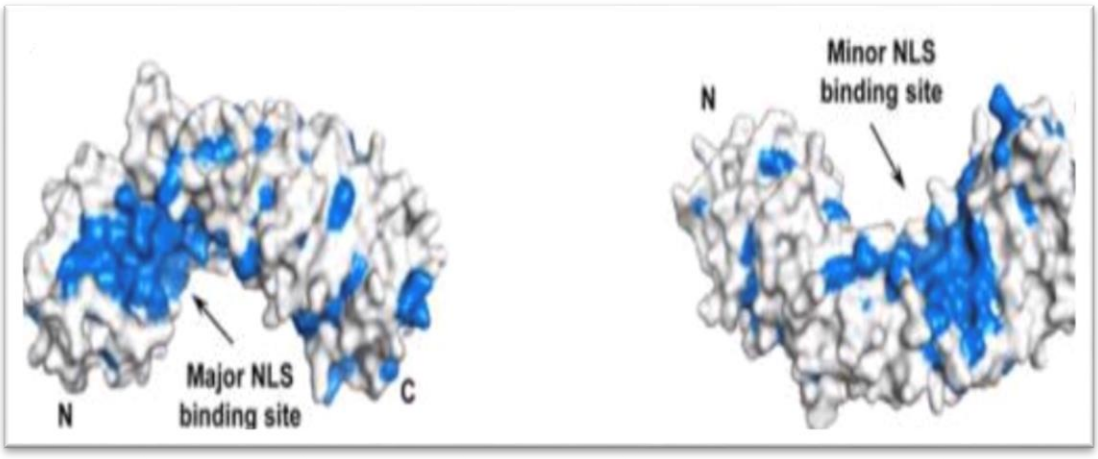


Figure 2.6 Importin α major and minor NLS-binding surface [96].

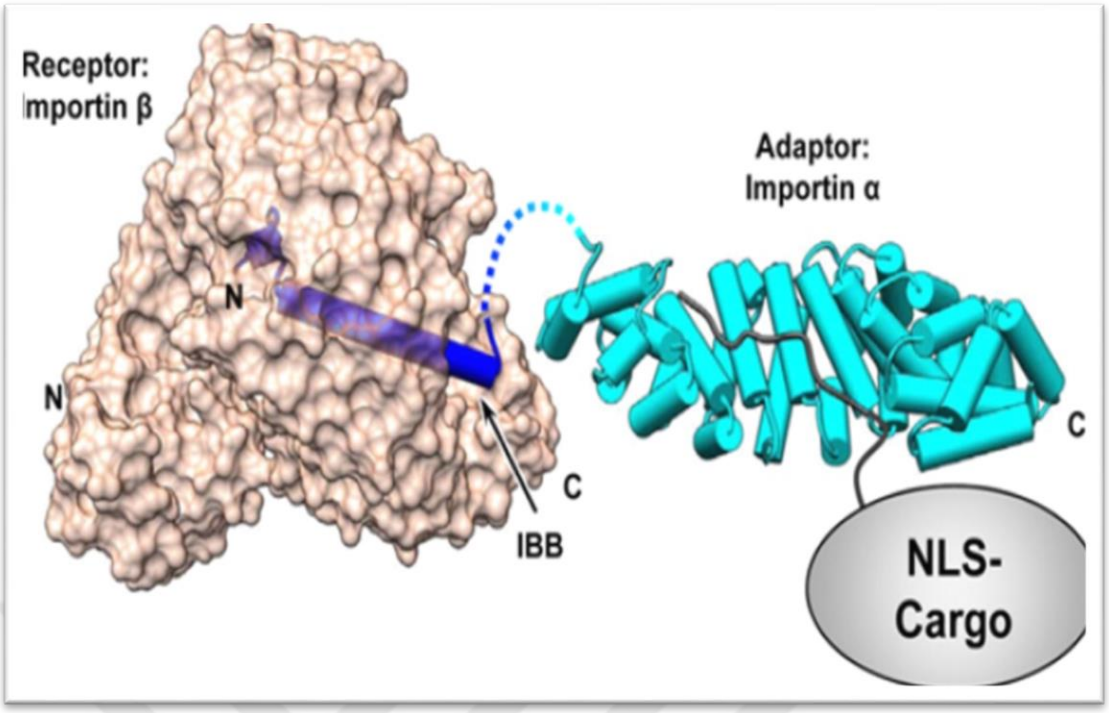


Figure 2.7 The classic nuclear import complex [96].The diagram is based on the structure of human importin β (beige) bound to the IBB domain (dark blue) and mouse importin α linked to the nucleoplasmin NLS (grey). The N-terminus and C-terminus of each structure are noted with an 'N' or 'C,' respectively. The illustration was produced using the Chimera program [109].

2.2.5 Nuclear Localization Signal (NLS)

2.2.5.1 Classical Nuclear Localization Signal

The import cycle begins when an importin-α differentiate the specific cargo protein from the other cellular proteins, Nuclear localization signal is a specific target sequence by which the transport protein can bind to the cargo protein and translocate it to the cell nucleus. For the import transportation, the best-identified transport signal is the classical NLS (cNLS), which consists of either one (monopartite) or two (bipartite) stretches of basic amino acids [11], [12]. Monopartite cNLSs are exemplified by the SV40 large T antigen NLS (^{126}PKKKRRV^{132}), and bipartite cNLSs are illustrated by the nucleoplasmin NLS (^{155}KRPAATKKAGQAKKKK^{170}) (Table 2.3). Monopartite NLS contains consecutive residues of N-terminal lysine; these residues are called P1, P2, etc. [11], [12]. The key requirements for the classical NLS were identified in several structural [97],[110] and thermodynamic [111] studies. In these studies it was shown that P1 position should contain a lysine followed by basic residues in positions P2 and P4, this implies that the monopartite NLS sequence requires a consecutive sequence of

K (K/R) *X* (K/R). Additionally, *in vivo* and *in vitro* alanine scanning of the Myc, monopartite SV40, and the pre-designed bipartite SV40 showed that the binding affinity of cNLS for importin- *α in vitro* is the same as the binding affinity for importin-*α in vivo*, they even share the same steady-state nuclear accumulation and import rate for the same cNLS cargo protein [111],[112]. Putting the obtained results into consideration, the functional binding capability of cNLS was determined, for each cNLS was found to have a binding capacity of ~10 nM for importin-*α* [112]. Non-functional near-cNLS sequences can bind too weakly or too tightly to the importin-*α* protein, and this interaction will prevent the protein from being effectively imported to the nucleus or released from the receptor in the nucleus, Nup2, and Cse1 release factors can help detach these cargo proteins from importin-α [113]. The transport rate of the cNLS cargo was found highly dependable on how fast the importin complex is formed; this was indicated by recent computer simulations [74]. Therefore, two factors are responsible for the accumulation of cNLS inside the nucleus, one of them is attributed binding affinity of the cNLS to the importin-*α*, and the other is the concentration of the importin-*α* receptor itself [74], [112]. This interpretation explains the characteristics of other NLS cargo/receptor interactions [114].

Table 2.3 Examples of different types of nuclear localization signals.

NLS Type	**Protein**	**NLS Amino Acid Sequence**	**Reference**
Conventional NLSs	SV40 large T-Ag	PKKKRKV [132]	[10]
	Polyoma large T-Ag	VSRKRPRP [196]	[115]
	Hepatitis D virus antigen	EGAPPAKRAR [75]	[52]
	murine p53	PPQPKKKPLDGE [322]	[116]
	NF-κB p50	QRKRQK [372]	[117]
	NF-κB p65	EEKRKR [286]	[118]
	Human c-myc	PAAKRVKLD [328] / RQRRNELKRSF [374]	[119]
Bipartite NLSs	*Xenopus* nucleoplasmin	KRPAATKKAGQAKKKKLD[171]	[120]
	Rat glucocorticoid receptor	YRKCLQAGMNLEARKTKKKI KGIQQATA[524]	[121]
	RCC1	MSPKRIAKRRSPPADAIPKSKK VKVSHR [28]	[122]
Arginine rich NLSs	HTLV-1 Rex protein	MPKTRRRPRRSQRKRPPT [18]	[123]
	HIV-1 Rev protein	RQARRNRRRRWR [46]	[124]

Table 2.3 Examples of different types of nuclear localization signals. (Continued)

Atypical NLSs	Matα2	MNKIPIKDLLNPQ [13]/ VRILESWFAKNI [159]	[125]
	Hepatitis B virus core antigen	SKCLGWLWG [29]	[126]
	Human rpL23a	VHSHKKKKIRTSPTFTTPKTLRL RRQPKYPR-KSAPRRNKLDHY [74]	[127]
	Human hnRNP A1	NQSSNFGPMKGGNFGGRSSGPY GGGGQ-YFAKPRNQGGY [305]	[128]
	SREBP2	RSSINDKIIELKDLVMGTDAKMH KSGVLRK-AIDYIKYLQQVNHKLRQENMVL KLANQKNKL[403]	[129]

2.2.5.2 The Importin α/cNLS Interaction

X-ray crystallography techniques illustrate the interactions between importin-*α* and cNLS [97],[110]. Figure 2.8 A dissects the importin-*α* conformation which comprises three *α*-helices, binding, and dissociation domain located in the N-terminal called (the IBB domain) recognizes importin-ß and compartmentalize the cargo protein .[130], [131], [132]. Importin-*α*, as mentioned before, contains two pockets, major and minor these pockets mainly consist of tryptophan and asparagin [88],[133]. The lysine side chains of the cNLS then embed itself in the groove and form salt bridges between the hydrophobic consecutive tryptophan side chains with a negatively charged residues, where the main chain interaction is made by the asparagine [88],[133].

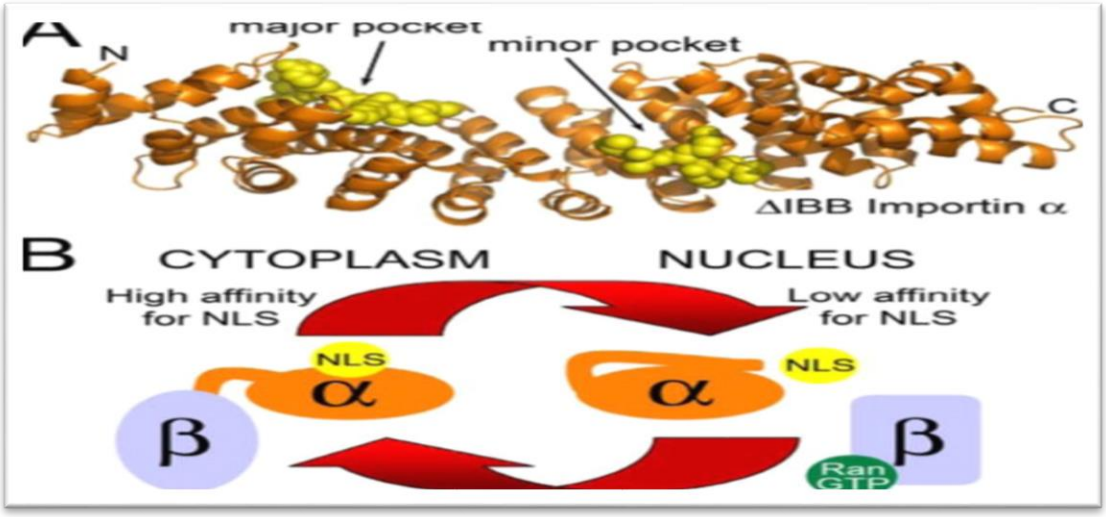


Figure 2.8 A, The interaction between importin-α and the classical nuclear localization signal. B, the effect of the autoinhibitory region on the N-terminal importin-α.

Inside the structure of importin-*α*, there is a region called the autoinhibitory region responsible for maintaining the cNLS translocation to the cell nucleus by particularly competing for binding with all cNLS. This region makes the delivery more specific and efficient [88],[133] as shown in Figure 2.8B.

This autoinhibitory region was located in the N-terminal region of importin-*α* and represented by KRR residues [131] that mimic the basic cNLS. After passing through the nuclear pore complex, the NLS-importin-α-importin-β disassociate in several stages. First, importin-α is released by importin-β. Second, the free N-terminal of importin- α reshape itself to interact with major cNLS binding groove [88],[133],[134]. Finally, the autoinhibitory region in the N-terminal will affect the bond between importin-α mono-partite and bipartite cNLS which on its turn will release the transported protein into the nucleus, because the mono and bipartite bind usually to the major pocket, and this indicates that the autoinhibitory region works as a regulator for the transport mechanism [88],[133], [134].

2.2.5.3 Non-classical Nuclear Localization Signal

Non-classical nuclear localization signal is an amino acid sequence that was found to function in nuclear import [103], [135],[136]. It is called non-classical because it does not bind to the same pocket with importin-α as the mono and bipartite cNLS [87]. Recent cell biological studies supported the claim that ncNLS are also necessary and effective in the nuclear import, it means that not only the cNLS is required in the import mechanism, but the ncNLS can also affect the binding of nucleoproteins and importin-α [103], [135],[136]. These studies showed that some alterations in the basic residues of ncNLS severally changed the nuclear import of the nucleoprotein [135],[136]. Another proof, in GST pull-down assays it was found that the binding ability of the protein to the importin-α was decreased remarkably because of these alterations [136]. Some cells exhibited a nuclear import defect caused by ncNLS peptide but not by cNLS [136]. Pull-down assays showed that there was a defect in the binding ability caused by a ncNLS peptide not SV40 NLS [136]. In the X-ray crystal structures of NP [137],[138], the N-terminal of the nucleoprotein is disordered and protrudes out of the folded domain, indicating that the ncNLS of free nucleoprotein are accessible for importin-α binding [137],[138].

Previous studies HNF1A protein mutations exhibited impaired nuclear localization. R217 is a positively charged amino acid which constructs the N-terminal cluster of nuclear localization signal like, region C (271-288), it was found that the mutations in region C such as R271W cause defective nuclear localization and the proteins were found accumulated in the cytoplasm [1]. A functional analysis study was conducted for p.Ser345Tyr candidate mutation which was located in the non-classical nuclear localization signal of HNF1A-MODY3 gene. In these studies, the localization of Ser345Tyr mutant HNF1A protein to the c nucleus was found to be defective.

CHAPTER 3

MATERIALS AND METHODS

3.1 Materials

3.1.1 Equipments

- Deep freeze (-80°C) : New Brunswick (Model U4100)
- Refrigerator (-20°C, +4°C): Arçelik
- Ice machine: Scotsman (Model:AF 80, USA)
- Microwave oven: Arçelik (Model: MD564, TR)
- Vortex: Dragon Lab (Model: MX-S)
- Water bath: Wisd (Model: 1068)
- Incubator: Nüve (Model: EN 400)
- Incubator shaker: Heildoph (Model: Unimax100)
- CO_2 incubator: MMM Group (Model: LSIK/ICV111)
- Inverted light microscope: Olympus (Model: CKX41)
- Thermal cycler: BioRad (Model: T100)
- UV imaging device: UVITec Cambridge
- Microcentrifuge: Sigma (Model: 1-15PK)
- Highspeed centrifuge: Beckman CoulterModel: Allegra X-30R and 64R
- NanoDrop 2000 spectrophotometer: Thermo Scientific (Model: NanoDrop2000)
- Spectrophotometer: Jenway (Model: 6300/05/20D)
- Hemocytometer: Sigma-Aldrich (Model: Z359629)
- Biosafety cabinet: TezSan (Model: Class II)
- Autoclave: Nüve (Model: OT 40L)
- Magnetic stirrer: Wisd (Model: MSH-20A)
- Dry bath incubator: Major Science (Model MC-01N-01S)

- pH meter: Hanna Instruments (Model: HI2211)
- Distilled water system: ELGA (Model: Purelab Option-Q, DV25)
- iblot™ gel transfer device: Invitrogen (Model: IB1001EU)
- Powerease® 90W: Life Technologies (Model: PS0091)
- Bolt™ mini gel tank: Life Technologies (Model: B4477599)

3.1.2 Cell Lines

Cell lines used in the study are shown in Table 3.1.

Table 3.1 Cell lines

Cell line	Company	Type	Origin
Cos-7	AddexBio	Cercopithecus aethiops (African Green Monkey)	Kidney fibroblast
Min-6	AddexBio	Mus musculus	Pancreas islets

3.1.3 Chemical Materials and Antibodies

- Bolt 4-12% Bis-Tris plus: Life Technologies.
- Iblot® gel transfer stacks nitrocellulose, Regular: Life Technologies.
- IBlot® DNA transfer Stack: Life Technologies,
- Seeblue plus prestained protein standard: Life Technologies,
- Bolt™ sample reducing agent (10X): Novex.
- LDS sample buffer (4X): Novex.
- Goat serum: Life Technologies.
- Acrylamide/Bis 19:1, 40% (w/v) solution: Life Technologies.
- TEMED: Life Technologies.
- APS: Life Technologies.
- DAPI: Life Technologies.
- Ethanol: Sigma-Aldrich
- Isopropanol: Sigma-Aldrich
- DMSO: Sigma-Aldrich
- HCl: Applichem.
- NaOH : Applichem
- Ampicillin: Sigma-Aldrich

- PBS: Gibco
- Trypsin-EDTA: Gibco
- DMEM: Gibco
- Opti-MEM: Gibco
- FBS: Gibco
- L-glutamine: Gibco
- Penicilin/Streptomycin, Gibco
- B-Mercaptoethanol, Gibco
- Tween-20, AppliChem
- BSA, AppliChem
- Skimmed milk powder, OXOID
- Agar, Merck
- Tris, Amresco
- Boric Acid, Merck
- EDTA, Applichem
- Rabbit polyclonal HNF1A antibody, Santa Cruz
- Mouse monoclonal Octa (FLAG) Antibody, Santa Cruz
- Goat anti-rabbit-HRP linked, Bio Rad
- Goat anti-mouse-HRP linked, Bio Rad
- Goat anti-rabbit Alexa-647, Life Technologies
- Goat anti-rat Alexa-488, Life Technologies
- Silencer pre-designed siRNA, Kpna6, Thermo Fisher
- Silencer Select Negative siRNA, Thermo Fisher

3.1.4 Primers

The primer pairs used in the *in vitro* mutagenesis study are shown in Table 3.2, and the primer pairs used for plasmid construction are shown in Table 3.3.

Table 3.2 Primer pairs used for *in vitro* mutagenesis study.

Variation	Primer sequences
p.R271W (**C**GG→**T**GG)	F:5'GCTCCTGGCGGCCCTGCT**C**GAGTCAGGGCTGAGCAAAG3' R:5'CTTTGCTCAGCCCTGACTCGA**G**CAGGGCCGCCAGGAGC3'

Table 3.3 Sequences of the primer pair used for plasmid construction.

Primer name	Primer sequences	Explanation
cDNA_HNF1A_2	F: 5'-TACAACTGGTTTGCCAACCG-3' R: 5'-CTGTGTTGGTGAACGTAGGAC-3'	Was used to confirm the p.R271W alteration on the HNF1A plasmid

3.1.5 Used Strains

For the expression vectors amplification, Escherichia coli DH5α strain [F-, φ80dlacZ_M15, _ (lacZYA-argF) U169, deoR, recA1, endAl, hsdR17 (rk-, mk +), phoA, supE44, λ-, thi-1, gyrA96,] was used.

3.1.6 Liquid and Solid Media

LB medium: 10 g of tryptone, 5 g of yeast extract and 10 g of NaCl were dissolved in 1 L of water and sterilized at 121 ° C for 15 min. Ampicillin was added to ensure that only the cells with ampicillin resistant gene live.

LB agar medium: 10 g of tryptone, 5 g of yeast extract, 10 g of NaCl and 15 g of agar were dissolved in 1 L of water and sterilized at 121 °C for 15 minutes. Ampicillin/kanamycin was added to differentiate the plasmid containing cells. About 30 ml of the LB agar medium was poured into the Petri dishes and cooled in the refrigerator.

COS-7 culture medium: DMEM containing 10% FBS, 2 mM L-Glutamine and 1% Pen / Strep was sterilized by filtration through 0.2 μm filters.

COS-7 freezing medium: 10% DMSO was added to the cells in complete DMEM and frozen at -80 ° C.

Min-6 culture medium: 15% FBS, 2 mM L-Glutamine, 1% Pen / Strep and 400 mM B-Mercaptoethanol in DMEM were added and sterilized by filtration through 0.2 μm filters.

Min-6 freezing medium: 10% DMSO was added to the cells in complete DMEM and frozen at 80 ° C.

3.1.7 Vectors

The expression vector (pCMV6b) containing human wild-type HNF1A cDNA (1.9 kb) was obtained from Prof. Dr. Eiji Kawasaki (Nagasaki University, Japan). The expression vector was regulated by the cytomegalovirus (CMV) promoter. FLAG-tagged pCMV-Tag 2 vectors used in co-immunoprecipitation study were provided by Jun Aruga (RIKEN Brain Science Institute, Japan). Human importin α transport proteins (importin α1, α3, and α7) have been studied with mouse homologous Kpna 2, 4 and 6 due to their sequence similarities and preserved structure. The map of the pCMV-Tag 2 vector containing the Kpna (Karyopherin-α) 2, 4 and 6 genes is shown in Figure 3.1, the vector's multiple cloning site regions (MCS) and the promoter region are shown in Figure 3.2.

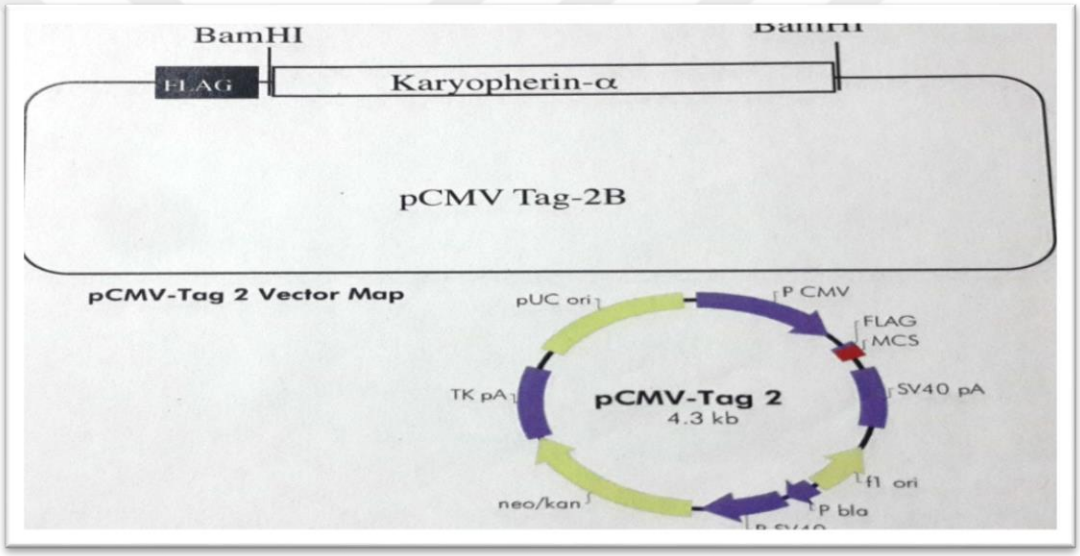


Figure 3.1 Mapping of the pCMV-Tag 2 vector.

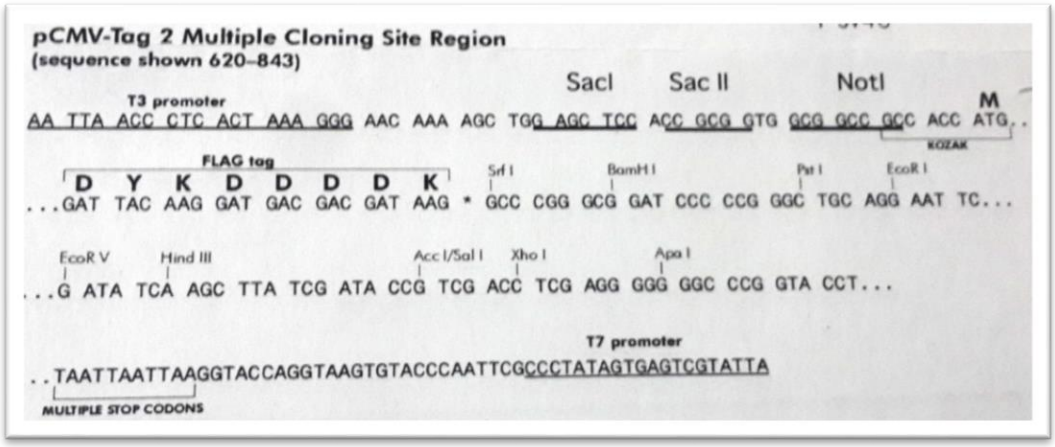


Figure 3.2. Multiple cloning site and promoter regions of the pCMV-Tag 2 vector.

3.1.8 Kits Used In This Study

- Quickchange II site-directed mutagenesis: Agilent.
- Lipofectamine 3000 transfection Reagent: ThermoFisher Scientific.
- Lipofectamine RNAimax transfection reagent: ThermoFisher Scientific.
- Plasmid isolation midi kit: Macherey-Nagel.
- Opti-4CN™ substrate kit: BioRad.
- Amplified Opti-4CN substrate kit: BioRad.
- Dynabeads® Protein G immunoprecipitation kit: ThermoFisher.
- Mammalian cell extraction kit: Biovision.

3.1.9 Buffers and Solutions

10X TBE buffer: 10X TBE buffer consists of 900 mM Tris Base, 900 mM Boric acid and 20 mM EDTA in distilled water. The 0.5X TBE buffer was used for DNA gel preparation and for buffering the gel electrophoresis tank.

Ampicillin solution (100 mg / mL): 1 g ampicillin is dissolved in about 9 mL of autoclaved water, and autoclaved water is added to make a final volume of 10 mL, filtered through 0.22 micron.

Kanamycin solution (100 mg / mL): Approximately 9 mL of 1 g kanamycin is dissolved in autoclaved water, and extra autoclaved water was added to make a final volume of 10 mL, the solution was filtered through 0.22-micron filter.

3.2 Methods

3.2.1 Mutant Plasmid Construction By *in vitro* Mutagenesis

The expression vector containing human wild-type HNF1A cDNA (1.9 kb) was regulated by the cytomegalovirus (CMV) promoter. "Quickchange II site-directed mutagenesis, Agilent Technologies" kit was used with the "*in vitro* mutagenesis" technique to generate R271W mutation (**C**GG→**T**GG) on the wild-type HNF1A. S345Y HNF1A cDNA mutations used in the project were created under the 3501-Career Development project. Synthesis reaction of the mutant sequences as described in Table 3.4 were prepared in a 50µl volume.

Table 3.4. The chemicals required for the synthesis reaction of the mutant sequence in "*in vitro* mutagenesis" technique.

Chemicals	**Volume(µl)**	**Concentration**
10X reaction buffer	5	1X
Plasmid template (20ng)	1	-
Primer Forward (10pmol)	1,25	0,25 pmol
Primer Reverse (10pmol)	1,25	0,25 pmol
dNTP (10mMol)	1	0,25 mMol
Quick solution	3	-
PfuUltra HF DNA Polymerase (2.5U/ µl)	1	0,05 U
Total volume	**50**	

The resulted mutation was then amplified using PCR according to the program indicated in Table 3.5.

Table 3.5 PCR amplification conditions for the newly synthesized mutant DNA.

Segment	**Cycle**	**Degree (^{0}C)**	**Time**
1	2	95	1 minute
2	18	95	50 seconds
		60	50 seconds
		68	6 minutes
3	1	68	7 minutes

After the amplification reaction, 1 µL of Dpn I (10 U / µL) restriction enzyme was added to each mutagenesis tube to cut off the methyl parental (non-mutated) DNA, and the mutated DNA was left at 37 °C for 1 hour. For the transformation, "XL10-Gold Ultracompetent" cells in chitin were used. After the competent cells were thawed on ice, 2 µl β-mercaptoethanol was added, and the tube was mixed gently. Then the cells were incubated for 10 minutes on ice and gently mixed every 2 minutes during this process. Subsequently, 2 µl of the plasmid DNA digested with Dpn I was introduced into the competent cells and allowed to incubate on ice for 30 minutes. To enhance the transformation reaction, the cell + plasmid mixture was kept in the water bath at 42 °C

for 30 seconds and incubated on ice for 2 minutes. This mixture was then added to 500 µL of pre-heated LB medium at 42 °C, placed on a shaker at 225 rpm and incubated at 37 °C for 1 hour. The cells were then plated in Petri dishes containing ampicillin+LB agar and allowed to be incubated for >16 hours at 37 °C.

3.2.2 Plasmid Isolation

After the incubation, a single isolated colony was selected and allowed to grow in an ampicillin-containing solution for approximately 8 hours at 37 °C in 5ml LB medium at 300 rpm to generate the first culture. The colonized bacteria was then diluted 1: 1000 in 100 ml LB medium and allowed to grow overnight at 300 rpm at 37°C. Plasmid isolation was performed by using "Nucleobond xtraMidi, macherey-nagel" kit. The proliferated cells were then centrifuged at 6000 xg for 10 minutes at +4° C. The resulting supernatant was discarded, and the pellet containing the cells were dissolved in the "Resuspension buffer RES + RNAase" in 8ml of chitin. Then 8 ml of lysis buffer (Buffer LYS) was added, gently mixed and allowed to incubate at room temperature for 5 minutes. Columns were equilibrated with buffer (Buffer EQU) to completely moisten the filters in the columns provided by the kit. 8 ml of "Neutralization buffer" was then added to the cell mixture, gently inverted 10-15 times and transferred directly to the columns. The cell lysis was loaded on these columns and kept until the solution completely pulled down by the gravity.

After that, the filters were discarded, and 5ml washing buffer was added to the column. After gravity had drained the buffer entirely from the column, the step with the wash buffer was repeated. The column was then transferred into a new collection tube, and the elution buffer was then added to the column to separate the plasmid.

3.5 ml isopropanol was added at room temperature to precipitate the plasmid; the tube then was centrifuged at room temperature for 15 minutes at 5000Xg. The supernatant was discarded, and the plasmid DNA in the pellet washed with 2 ml 70% ethanol. It was then centrifuged at 5000Xg for 5 minutes, and the ethanol fraction was carefully discarded. The pellet was allowed to dry in the air for 10 minutes. Plasmid DNA was then dissolved in 30 uL of TE buffer. Plasmid concentrations were measured on the Nanodrop device. DNA sequencing was performed to confirm the generated DNA sequences by *in-vitro* mutagenesis method. PCMV-Tag 2 vectors containing FLAG-

tagged Kpna2, 4 and 6 genes were amplified in LB agar Petri dishes containing kanamycin and sent to DNA sequence analysis for validation.

3.2.3 Cell Culture Studies

The co-immunoprecipitation assay was carried out by using cell line without endogenous expression of HNF1A (COS-7 cells), silencing with siRNA and immunolocalization was accomplished by using cell line with the endogenous expression of HNF1A (Min6 cells). COS-7 and Min6 cells were grown using different DEMEM.

COS-7 and Min6 cells were dissolved after taking them out of the -80 C freezer, 9 ml of DEMEM were added to the stocked cells in a 50 ml falcon tube and centrifuged for 10 min at 3000 rpm, The supernatant was then removed and 5 ml of complete DMEM was added to homogenize the suspended cells. Resuspended cells were cultured on T-25 flasks and incubated at 37C and 5% CO_2. DMEM was changed 2-3 times a week.

Adherent COS-7 and Min6 cells were passaged when 80-90% confluent. First DMEM was removed, and 5ml 1XPBS was added to wash. 1XPBS was discarded, 1ml Trypsin / EDTA was added to detach the cells. The cells were incubated at 37C for 5 minutes to speed up the cell's uptake. The detached cells were collected by adding 5 ml of complete DMEM and placed in a 50 ml Falcon tube and centrifuged for 5 minutes at 2500 rpm to precipitate the cells. The supernatant was then discarded, the palette was washed and homogenized with complete DMEM by pipetting. The proliferated cells were distributed in 6 or 12-well culture dishes according to the study method.

COS-7 cells were transfected using "Lipofectamine 3000 transfection reagent, Thermo Scientific". In 6-well plate the 350000 COS-7 cells were prepared 24 hours at 80-90% confluency prior to the transfection. Plasmids containing wild or mutant type HNF1A and Kpna (2, 4 or 6) genes in the volumes indicated in Table 3.6 were diluted in DMEM in appropriate culture dishes for co-immunoprecipitation studies. This mixture was then added to the "Lipofectamine 3000 Transfection Reagent" as referred in Table 3.6 and incubated at room temperature for 20 minutes. After taking the 6-well culture plate out of the incubator, the Lipofectamine 3000 and plasmid mixture was distributed by pipetting to the 6-well plate dropwise to the entire surface. As a control, only the Opti-MEM + reagent mixture was added to one well. For siRNA silencing and

immunolocalization studies, Min-6 cells were cultured 24 hours prior to siRNA transfection, 20,000 cells per well were selected and added to 6-well cell dishes.

3.2.4 Co-immunoprecipitation Study

The co-immunoprecipitation study was performed to determine which importin α subset is responsible for the transfer of wild-type HNF1A protein to the cell nucleus and to analyze the binding ability of specific importin α proteins and mutant HNF1A proteins (R271W and S345Y). For this study, 350,000 Cos-7 cells were allowed to grow in 6-well culture dishes at least 24 hours at 70-90% confluency prior to the transfection. "Lipofectamine 3000 transfection reagent for transfection, Thermo Scientific" was used in the volumes indicated in Table 3.6.

Table 3.6 Transfection reaction conditions and steps

1 (A)	Lipofectamine 3000 reagent	7,5 µl / per well
	Opti-MEM	125 µl / per well
2 (B)	DNA #	2,5 µg / per well
	Opti-MEM	125 µl / per well
	P3000 reagent	5 µl / per well
3	Components in tubes A and B were mixed in equal proportions and incubated for 15 minutes at room temperature.	
4	At the end of 15 minutes, the mixture was added dropwise to the cells in the 6-well plates 1 day in advance, and the results were analyzed at the end of the 2-day waiting period.	
#	The expression vector containing the 1,25 wild-type and mutant HNF1A gene and the expression vector containing the 1.25 µg Kpna2, 4 or 6 genes were added.	

3.2.4.1 Total Protein Extraction

48 Hours after transfection, the "Mammalian cell extraction kit, Biovision" was used to obtain total protein from the cells. Every stage of cell disruption was done on the ice. COS-7 cells grown in 6-well culture dishes were taken out of the incubator, placed on ice, and the complete medium (DMEM) was removed. The cells were then washed once with 1 ml of 1X PBS on the ice, and then the whole PBS was pipetted. By adding 1 ml of PBS to each well, the cells were separated from the culture dish using cell scratcher,

and transferred to 1.5 ml microcentrifuge tube. The collected cells were centrifuged at +4°C for 5 minutes at 600Xg. The supernatant was discarded and 100µl "Extraction buffer mix" was added to the cells, homogenized by pipetting and incubated on ice for 10 minutes. The mixture was then vortexed for 5 seconds and centrifuged at maximum speed for 3 minutes. The supernatant containing the whole cell lysate was carefully removed without lifting the pellet and transferred to a new microcentrifuge tube. Cell lysis was stored at -80 °C for later use in the co-immunoprecipitation study.

3.2.4.2 Co-immunoprecipitation Assay

Cell lysates obtained from Cos-7 cells were separated for 10 µl negative control and 20 µl for input. The negative control was used in this study to show that the magnetic beads would not bind to another similar protein in the cell lysate without the antibody. The lysate containing all cell proteins was used as input without entering the co-immunoprecipitation process. The input shows that vectors containing the transfected HNF1A and Kpna genes are successfully expressed inside the cell.

For the co-immunoprecipitation assay, 4 µg FLAG antibody was added to the cell lysates and incubated overnight at +4° C with rotation. The next day, magnetic beads (Dynabeads protein G, Thermo Scientific) in the tube were vortexed for 15 minutes, and 50 µl of the dynabeads were added to a new set of tubes (for negative control and for IP). The tubes were placed on magnet and the preserving buffer was removed. The beads were then washed with “Antibody binding and washing buffer” one time, and put on magnet to remove the buffer. Then, the beads were added to the FLAG antibody-cell lysate mixture (which was incubated overnight) along with the “Antibody binding and washing buffer”. Lysate + antibody + magnetic beads + AB buffer mixture was placed on the rotator for 2 hours. Same procedure was done for the negative control tubes, but the beads were only added to the cell lysate, without the antibody.

Subsequently, the tubes were placed on magnet and the supernatant (unbound proteins) was removed. The beads were washed three times with 200 µl of "washing buffer" solution provided with the kit. At each step, the beads were gently washed, and the supernatant was removed inside the magnetic field. At the final step, 100µl of "washing buffer" was added to transfer the isolated protein with the magnetic beads to a clean set of tubes. The tubes were then placed on the magnet, and the supernatant was removed. The mixture containing the magnetic bead-lysate-antibody (IP tubes) was gently dissolved in 20 µl of "elution buffer" provided by the kit. With the help of the magnetic

field, the supernatant containing precipitated proteins was carried out into clean tubes to prepare them for western blot analysis. Same steps were also done for the negative control tubes.

3.2.4.3 Western Blot Analysis

Western blot analysis was performed using the "Bolt welcome pack IBLOT, Invitrogen" system containing electrophoresis and transfer device. The isolated proteins from the co-immunoprecipitation assay, the negative control, and the input were loaded to the gel for Western blot analysis and prepared at the measurements indicated in Table 3.7. Accordingly, the proteins in each tube were denatured at 70° C for 10 min.

Table 3.7 Volumes needed for the protein samples to be loaded to the gel.

Sample (µl)	**LSD sample buffer (4X) µl**	**Sample reducing agent (10X) (µl)**	**dH_20(µl)**	**Total volume (µl)**
20	10	4	6	40

12% SDS-polyacrylamide resolving gel and 4% stacking gel were prepared for Western blot analysis as described in Table 3.8.

Table 3.8 Volumes needed for preparing 12% and 4% SDS-PAGE

Solution	**12% PAGE (Resolving gel)**	**4%PAGE (Stacking gel)**
SureCast acrylamide (40%)	2.4 ml	0.30 ml
SureCast resolving buffer	2 ml	0.75 ml
Distilled water	3.5 ml	1.92 ml
10% SureCast APS	80 µl	30 µl
TEMED	8 µl	3 µl
%12 PAGE was prepared and added to the space between the glasses until the line in the glass was reached then %4 PAGE was added, and a comb-like plastic was inserted between the glasses to form the wells.		

Protein samples and protein marker were loaded into the prepared SDS-PAGE, run in 1X MES running buffer at 165V for 1.5 hours. The gel was then removed from the glass

plates, transferred to the gel transfer device for dry transfer and a 7-minute program was applied to the membrane. After the translocation of the protein bands from the gel to the membrane, the gel was removed from the device and membrane cutting was performed from the appropriate site where the HNF1A and Kpna protein bands will appear. The membrane was then washed twice with PBST for 5 minutes. At the end of the washing steps, the membrane was incubated with shaking for 1 hour in a 5% milk powder solution for blocking. After blocking, the membrane was washed twice with 1XPBST for 5 minutes.

For the analysis of HNF1A protein, the primary antibody was “Rabbit anti-HNF1A” while HRP-conjugated "Goat-anti-rabbit, Santa Crus” was used as the secondary antibody. The primary antibody was prepared using 1XPBST and BSA (1%) as 1: 250 dilution, while the secondary antibody was 1: 5000 dilution. Monoclonal mouse FLAG was used as the primary antibody, and HRP-conjugated "Goat-anti-mouse" was used as the secondary antibody for FLAG-tagged Kpna proteins. The membrane was incubated with the primary antibody dilution for 1 h at room temperature for imaging of HNF1A protein, Kpna containing membrane was incubated with the FLAG-tagged antibody for overnight at +4°C for imaging of Kpna protein. The membrane was then washed 3 times with 1XPBST for 5 minutes. The membrane was incubated with the dilution of the secondary antibody for another 1 hour at room temperature. The membrane was then washed 3 times with 1XPBST for 5 minutes.

Protein imaging was performed using the "Amplified Opti-4CN detection kit, Bio-Rad". For this, 8ml 1X BAR (4ml amplification diluent + 2ml BAR + 2ml distilled water) solution was prepared, added to the membrane and incubated with shaking for 10 minutes. The membrane was then washed 3 times with 20% DMSO / PBST and then 2 times with PBST for 5 minutes each. Streptavidin was prepared in 1% BSA / PBST as a 10 ml dilution, added to the membrane and incubated with shaking for 30 minutes. Then the membrane washed 2 times with PBST for 5 minutes. For the colorimetric imaging, 1ml Opti-4CN diluent was mixed with 9ml dH_2O. This mixture was added to the 200ul Opti-4CN substrate and poured over the membrane. The membrane was incubated with the substrate for 20 minutes until the protein bands were evidenced. The membrane was then washed with dH_2O for 15 minutes to stop the reaction.

3.2.5 siRNA Silencing and Immunolocalization Study

The co-immunoprecipitation assay showed that Kpna6 has the highest binding ability to HNF1A, so Kpna6 was silenced. The immunocytochemical analysis revealed that the

HNF1A protein was localized to the cell nucleus even after the Kpna6 knockdown. Silencing was carried out in mouse pancreatic cells Min6 using mouse Kpna6 protein-specific siRNA (Silencer pre-designed Kpna6 siRNA, Thermo Fisher). As a negative control, "Silencer select negative siRNA, Thermo Fisher" was used. Cells treated with siRNA were compared with untreated cells. In this study, it was also investigated whether HNF1A and Kpna6 proteins were co-localized in the cell nucleus by immunocytochemical analysis to confirm the results obtained by co-immunoprecipitation. To allow Min6 cells to grow on the coverslip, the poly-L-lysine coating was applied. For this procedure, each coverslip was covered with 100µl of poly-L-lysine (0.2mg / ml) in 12-well culture dish and allowed to stand at room temperature for 1 hour. Each coverslip was then washed 6 times with distilled water for 5 minutes. The coverslip was left to dry and kept at room temperature under sterile conditions.

3.2.5.1 Silencing With siRNA

For immunocytochemical staining, Min6 cells grown in T-25 flasks were first passaged after 24 hours in 6-well culture dish, and 20,000 cells were allowed to grow on the coverslip of each well. After 24 hours, Min6 cells were transfected using Kpna 6 specific “siRNA Lipofectamine RNAimax Transfection Reagent Thermo Scientific." The volumes were added according to the recommended instructions provided by the kit, and transfection solutions were prepared as described in Table 3.9. Cell medium was changed 24 hours after transfection. 48 hours later the cells were prepared for immunolocalization study.

Table 3.9 siRNA transfection reaction conditions and steps.

1 (A)	Lipofectamine RNAimax reagent	9 µl / per well
	Opti-MEM	150 µl / per well
2 (B)	siRNA / Negative control siRNA (10µmol)	3 µl (30pmol) / per well
	Opti-MEM	150 µl / per well
3	Chemicals in tube A and B were mixed evenly and incubated for 5 min at room temperature	
4	By the end of the 5th minute, the mixture was added drop-wise to the cells grown on the coverslip inside the 6-well culture dish and incubated for 1 day in advance; the results were analyzed at the end of the second day.	

3.2.5.2 Immunocytochemical Staining Assay

After 48 hours the cells were fixed using methanol. For this procedure, the supernatant was first removed from the wells, and 1 ml of methanol (100%) was added to each well and kept at -20 °C. The culture dish then stored at -20 °C for 10 minutes. The methanol was then removed, and the cells were washed 3 times with 1XPBS for 5 minutes. Until the day when immunocytochemical staining was performed, the cells were kept in 1X PBS at 4 °C. Prior to staining, PBS was removed from the cells and blocking was performed. For this procedure, 5ml blocking solution (10% Goat serum in 1X PBS, 10mg / ml BSA) was prepared. 350 µl of blocking solution was placed in each well and incubated at room temperature for 1 hour. The primary antibody for HNF1A (polyclonal rabbit anti-HNF1A, Santa Cruz) and primary antibody for Kpna6 were prepared in 1XPBS-1% BSA in a 1: 250 dilution, 300 µl of each antibody was added to each well, and the cells were left overnight at 4°C. The next day, the primary antibody solution was removed from the wells, and the cells were washed 3 times with 1X PBS for 5 minutes. After washing, the cells were incubated in 350 µl of blocking solution for 1 hour at room temperature. After removing the blocking solution from the wells, a mixture of secondary antibody diluted 1: 1000 in 1XPBS-1% BSA (Goat anti-rabbit/ Alexa-647) and 1: 1500 diluted secondary antibody (Goat anti-rat-Alexa-488) was added to the cells. By this staining, the HNF1A protein was red, and the Kpna6 protein was green. For the secondary antibody application, the cells were kept in the dark for 1 hour at 37°C. Cells washed 3 times with 1XPBS for minutes and stained with DAPI diluted 1: 1000 at room temperature for 10 minutes. DAPI will give blue radiation and was used to detect the cell nucleus. Cells were washed 3 times for 5 minutes with PBS, 10µL of mounting medium was added, and the coverslip was inverted and placed on the slide. The edges of the coverslip were closed using nail polish. The confocal microscopy study was carried out at the Department of Molecular Biology and Genetics at Boğaziçi University. The stained cells were imaged with a microscope 63X objective with a laser (excitation wavelength 405 nm for DAPI, excitation wavelength 653 nm for Alexa-647 and 495 nm for Alexa-488). The cells were analyzed using ImageJ software (https://imagej.net/Fiji).

CHAPTER 4

RESULTS

4.1 Verification of Mutant HNF1A and Kpna Expression Vectors

The variation of HNF1A R271W generated by the "*In vitro* mutagenesis" method was confirmed by the DNA sequencing method as shown in Figure 4.1.

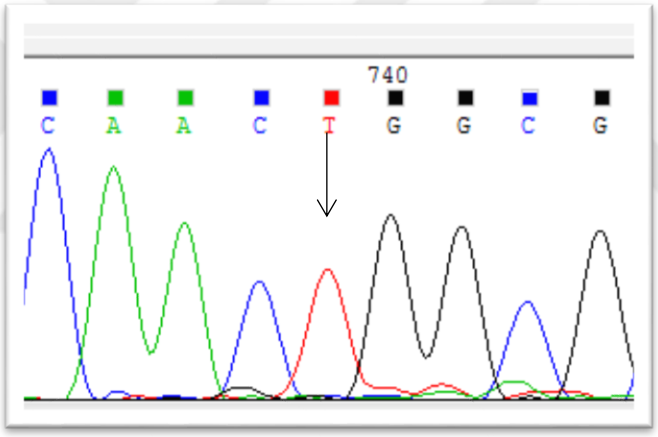


Figure 4.1 Verification of R271W (**C**GG→**T**GG) mutation generated by *in vitro* mutagenesis by DNA sequencing method.

Kpna2, 4, and 6 expression vectors were verified by DNA sequencing with primers specific for the T3 and T3 promoter. As shown in Figure 4.2, the Kpna genes were cloned into the BamHI restriction sites (G ^ GATCC) of the vector.

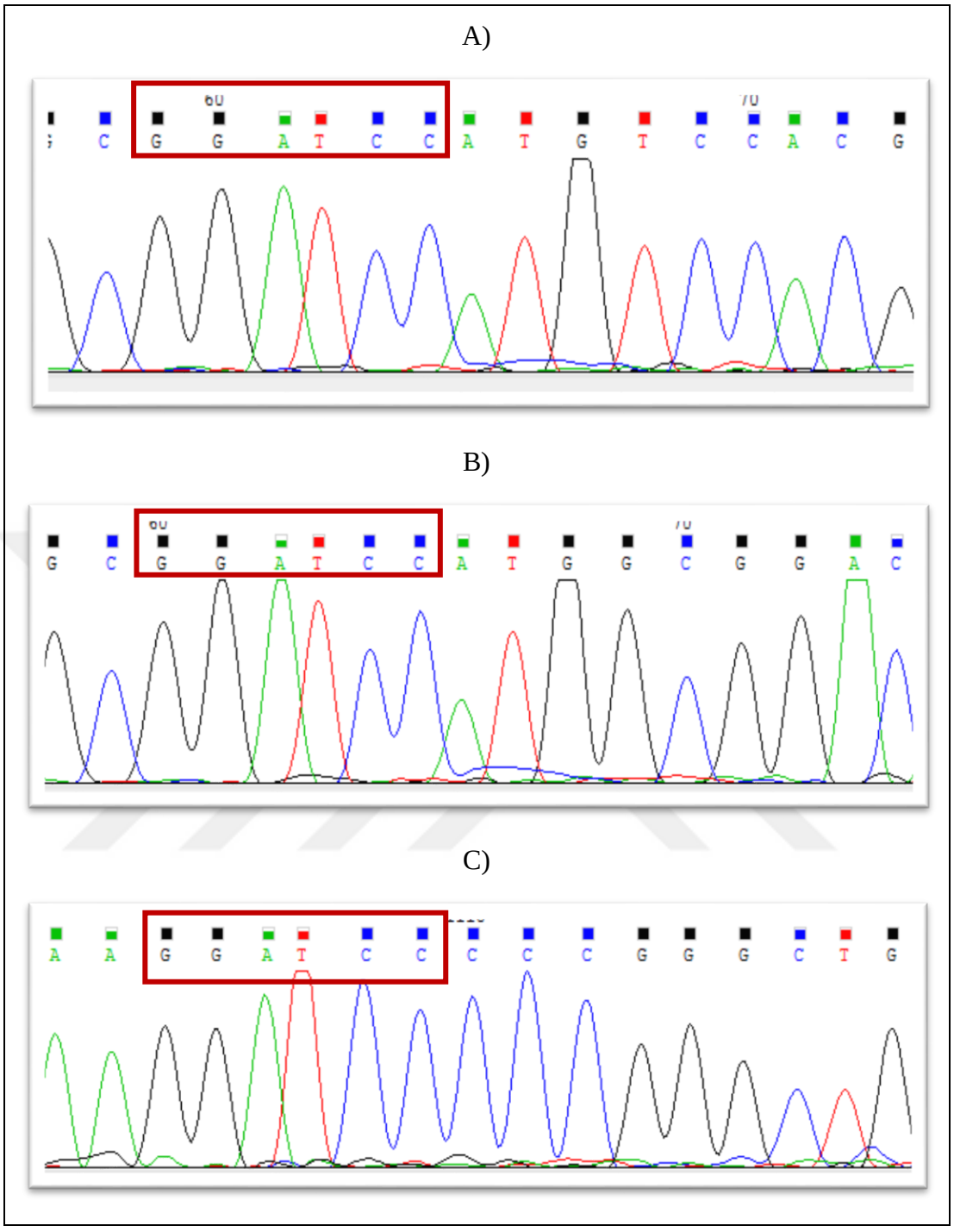


Figure 4.2 Confirmation of Kpna expression vectors by DNA sequence analysis. BamHI restriction sites in A) Kpna2 B) Kpna4 and C) Kpna6 expression vectors were indicated by red boxes.

4.2 Co-immunoprecipitation Assay of Wild-type HNF1A And Kpna Proteins in COS-7 cells

COS-7 cells without endogenous HNF1A expression were co-transfected with expression vectors containing wild-type HNF1A and Kpna2, 4 or 6 genes. The results of the co-immunoprecipitation assays were analyzed by Western blot analysis. The results are shown in Figures 4.3 and 4.4.

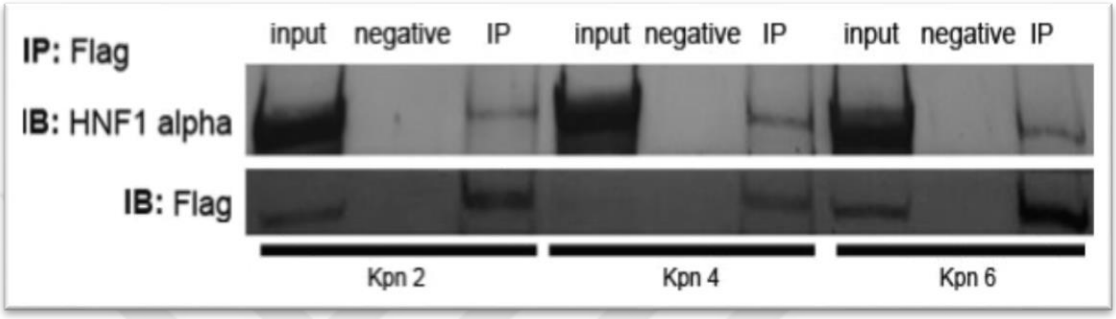


Figure 4.3 Results of the co-immunoprecipitation assay showing the interactions between wild-type HNF1A and Kpna 2,4 and 6 transport proteins. Input: indicates whole cell lysate, negative: magnetic beads and lysate without precipitating antibody, IP (Immunoprecipitation): Co-immunoprecipitation result, IB (Immunoblotting): Western blot.

Accordingly, mouse FLAG antibody was used to bind and precipitate FLAG-tagged Kpna 2,4 or 6 proteins. Western blot analysis was performed for protein analysis in precipitated cell lysates. HNF1A antibody and FLAG antibody were used as primary antibodies. In the input part, it was shown that both HNF1A and FLAG-conjugated Kpna2, 4 and 6 proteins were expressed successfully. The magnetic beads used in the negative control were used to confirm that there is no unspecific binding to another protein without the antibody being used for precipitation. As shown in Figure 4.3, it was observed that the HNF1A protein showed binding with all of the Kpna2, 4 and 6 proteins and precipitated together. Repeated co-immunoprecipitation studies (IP) showed that the strongest band was with Kpna6 protein as shown in Figure 4.4.

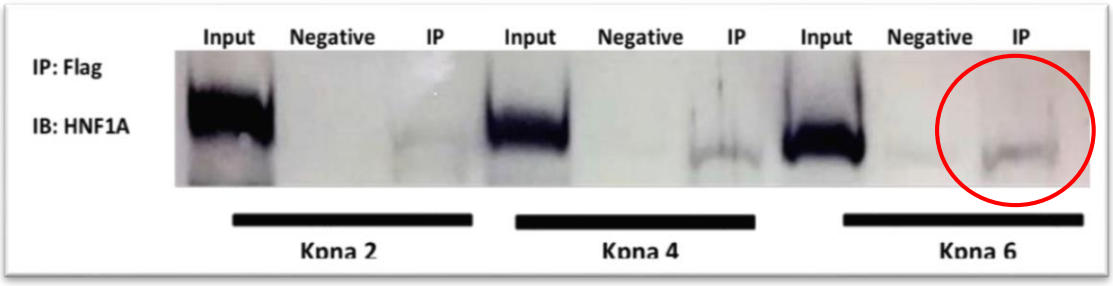


Figure 4.4 Results of the repeated co-immunoprecipitation assay. Input: whole cell lysate, negative: incubation of the lysate with magnetic beads without the participation of the antibody, IP (Immunoprecipitation): The result of the co-immunoprecipitation, IB (Immunoblotting): shows the primary antibody used in the Western blot part.

In addition, when the level of Kpna2, 4 and 6 proteins in the pancreas were compared in The Human Protein Atlas database, Kpna6 protein has the highest expression as shown in Figure 4.5. For these reasons, siRNA silencing and immunolocalization studies were carried out by selecting a Kpna6 protein-specific siRNA.



Figure 4.5 Expression levels of Kpna proteins in different tissues. The expression levels of A) KPNA2, B) KPNA4 and C) Kpna6 proteins in pancreatic tissue were indicated by red circle.

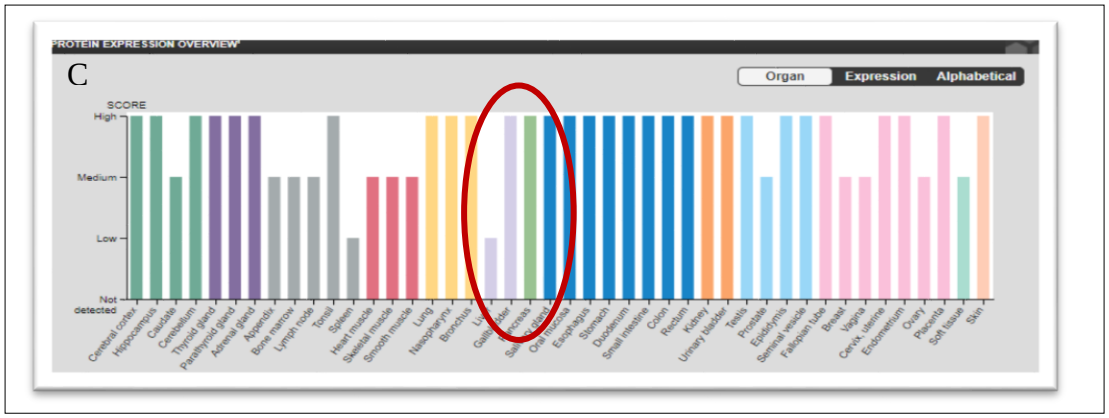


Figure 4.5 Expression levels of Kpna proteins in different tissues. The expression levels of A) KPNA2, B) KPNA4 and C) Kpna6 proteins in pancreatic tissue were indicated by red circle. (Continued)

4.3 Co-immunoprecipitation Assay With Kpna6 and Mutant HNF1A Proteins in COS-7 Cells

The Co-immunoprecipitation study with wild-type HNF1A and Kpna2, 4 and 6 proteins showed that the highest binding was with Kpna6 protein. The interactions of the Kpna6 protein with the mutant HNF1A (R271W and S345Y) proteins were investigated by the Co-immunoprecipitation assay and the Western Blot analysis. As shown in Figure 4.6, the mutant HNF1A proteins showed a decrease in the binding ability to the Kpna6 transport protein when compared to the wild HNF1A protein.

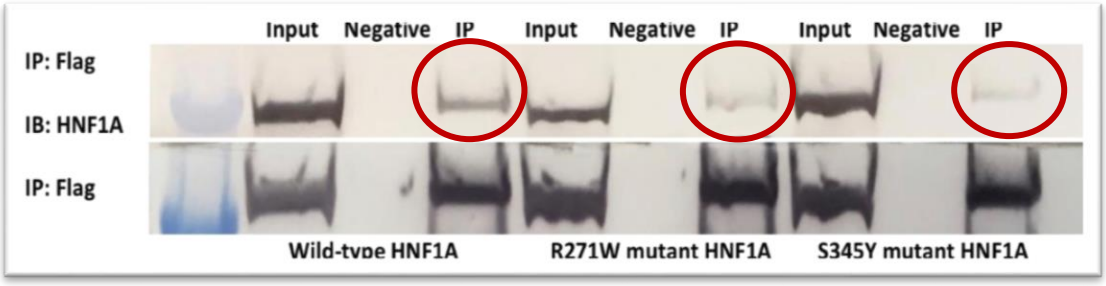


Figure 4.6 Co-immunoprecipitation results are showing the interactions between Kpna6 transport protein and wild and mutant HNF1A proteins. The red circles show Co-IP results. Input: whole cell lysate, negative: magnetic beads and cell lysate without precipitating the antibody, IP (Immunoprecipitation): co-immunoprecipitation result, IB (Immunoblotting): Western blot.

4.4 Downregulation of Mouse Kpna6 Transport Protein With siRNA and Immunolocalization Analysis Of HNF1A Protein in MIN6 Cells

Kpna6 transport protein-specific siRNA was transfected in mouse pancreatic Min6 cells. It was investigated by immunocytochemical analysis whether the localization of the wild HNF1A protein will be affected when Kpna6 protein (which showed the highest binding ability to the wild-type HNF1A) is downregulated.

4.4.1 The Effect of Kpna-specific siRNA on The Localization of HNF1A Protein in MIN6 Cells

As seen in Figure 4.7, no significant differences were found in the localization of HNF1A protein to the cell nucleus when siRNA treated cells were compared with none-treated ones. Control negative siRNA application showed similar results for HNF1A protein with cells that were not treated.

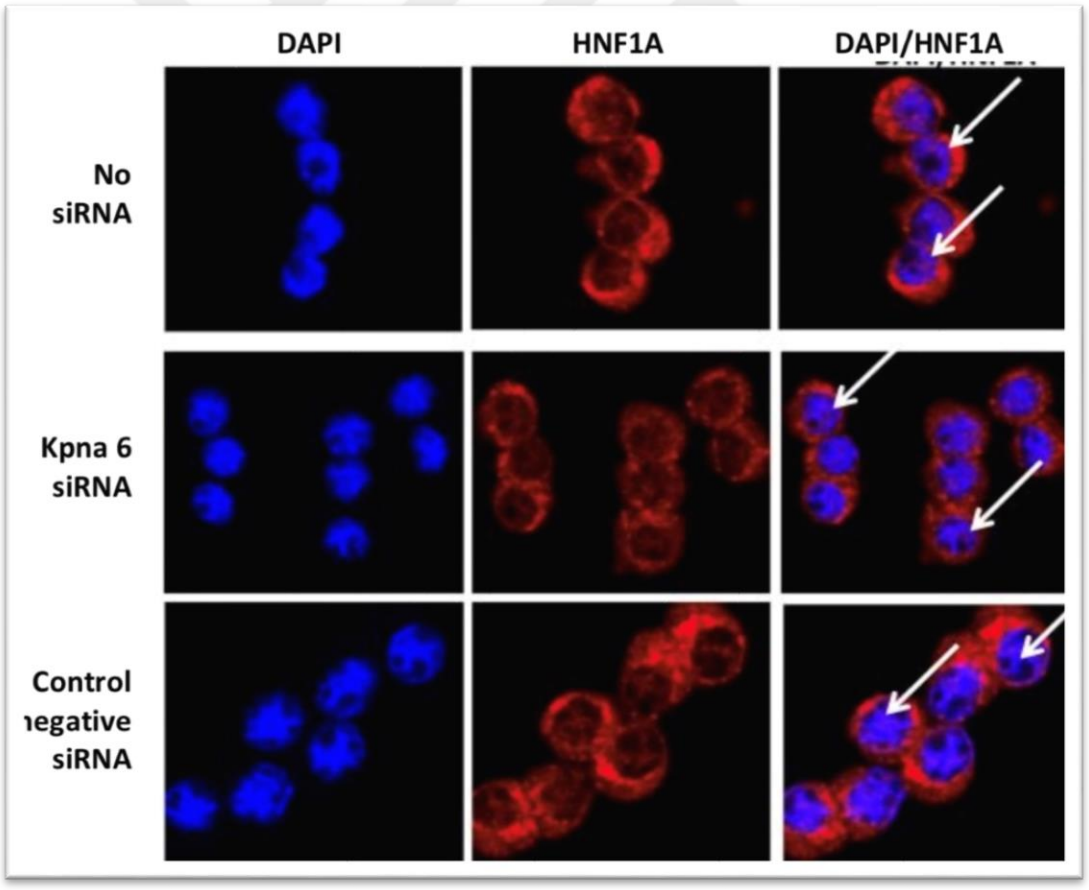


Figure 4.7 Nuclear localization of wild-type HNF1A transcription factors with Kpna6-specific siRNA and control negative siRNA-treatments. DAPI was used to stain the cell nucleus. HNF1A proteins localized in the nucleus were shown with arrows.

The effect of knockdown of Kpna6 on the nuclear localization of HNF1A protein was analyzed by ImageJ software in different cells. Areas of cells, mean signal amounts and standard deviation for HNF1A are shown in Table 4.1 and Table 4.2. Accordingly, the results obtained from the whole cell and only the cell nucleus without siRNA treatment for HNF1A protein are shown in Table 4.1, while the results of Kpna6-specific siRNA-treated cells are shown in Table 4.2. According to these results, 83% of HNF1A proteins in the whole cell were localized in the cell nucleus in non-siRNA treated cells, while 73% of the HNF1A protein in the whole cell was localized in the cell nucleus in siRNA–treated cells.

Table 4.1. Results obtained from the whole cell and the cell nucleus for HNF1A protein in non-treated cells.

	Cell nucleus		**Whole cell**	
Cell number	**Area (micron)**	**Average signal (pixels/micron)**	**Area (micron)**	**Average signal (pixels/micron)**
1	74.253	46.618	173.743	60.497
2	34.060	56.611	285.003	68.057
3	34.012	37.810	149.130	56.282
4	63.631	42.596	109.922	52.266
5	36.946	43.311	235.078	54.287
6	62.007	36.206	119.328	45.431
7	39.575	47.589	78.552	44.068
8	50.550	32.616	80.888	58.336
9	40.043	36.729	70.572	51.717
10	35.561	35.601	54.790	57.169
11	39.269	46.322	47.938	52.011
12	27.051	48.233	55.180	55.406
13	26.036	42.321	44.586	55.876
14	26.023	42.136	66.871	62.359
15	21.942	45.413	73.889	60.409

Table 4.1. Results obtained from the whole cell and the cell nucleus for HNF1A protein in non-treated cells. (Continued)

16	33.446	60.318	72.934	59.258
17	32.355	47.467	60.560	61.917
18	32.514	52.328	71.854	56.749
19	25.922	48.663	51.209	52.776
20	31.300	47.097	55.635	51.281
21	24.922	47.935	137.992	57.018
22	31.862	40.668	56.894	53.465
23	45.807	45.682	129.607	59.123
24	30.495	35.575	75.464	57.176
25	51.256	42.457	52.584	56.707
26	29.352	41.485	62.390	61.130
27	48.799	68.364	48.009	51.926
28	36.726	60.866	56.501	62.525
29	31.757	45.255	79.977	70.078
30	24.755	50.702	53.224	70.024
31	27.503	54.762	57.953	64.540
32	32.403	53.204	63.470	65.828
33	26.939	71.743	50.813	64.969
34	25.808	56.903	68.275	78.887
35	24.626	43.006	48.347	69.572
36	26.725	62.342	69.857	64.591
37	24.819	64.894	57.689	66.508
38	17.851	67.441	54.092	65.647
39	29.292	52.365	56.623	61.200
40	21.065	66.121	63.753	61.084

Table 4.1. Results obtained from the whole cell and the cell nucleus for HNF1A protein in non-treated cells. (Continued)

41	22.421	49.106	49.691	62.111
42	23.766	40.870	70.231	72.566
43	27.325	59.165	47.949	65.326
44	23.775	57.673	69.708	59.474
45	19.027	64.959	61.545	60.774
46	30.965	49.156	58.868	64.876
47	33.576	56.555	48.230	61.038
48	30.684	45.709	70.557	62.375
49	33.679	66.255	79.387	58.857
50	17.236	51.294	46.792	65.945
Mean	**32.838**	**50.117**	**78.083**	**60.230**
Standard deviation	11.399	9.694	46.807	6.693
Min	17.236	32.616	44.586	44.068
Max	74.253	71.743	285.003	78.887

Table 4.2 Results obtained from the whole cell and the cell nucleus for HNF1A protein in siRNA-treated cells.

	Cell nucleus		**Whole cell**	
Cell number	**Area (micron)**	**Average signal (pixels/micron)**	**Area (micron)**	**Average signal (pixels/micron)**
1	25.021	47.217	73.081	65.839
2	30.456	68.123	57.644	61.669
3	36.391	46.157	51.219	73.124
4	30.953	46.529	72.609	67.127
5	26.166	53.727	93.834	71.957
6	31.608	62.032	57.999	71.373

Table 4.2 Results obtained from the whole cell and the cell nucleus for HNF1A protein in siRNA-treated cells. (Continued)

7	28.364	58.308	48.775	73.148
8	28.445	57.654	57.682	70.114
9	29.208	67.435	81.151	87.858
10	20.800	43.673	54.116	70.051
11	20.852	49.774	35.538	57.790
12	28.429	65.155	43.203	69.114
13	26.162	58.339	54.486	66.936
14	23.566	52.359	50.879	61.622
15	24.394	56.171	72.972	63.724
16	21.527	48.762	57.838	65.059
17	34.682	48.797	51.461	62.044
18	29.921	37.962	77.244	60.218
19	38.646	39.740	61.646	51.076
20	42.167	30.815	67.167	48.093
21	40.335	28.792	108.852	50.487
22	40.312	32.066	108.711	47.942
23	41.698	33.305	117.981	47.392
24	38.546	39.711	100.328	45.638
25	44.514	29.179	91.038	56.909
26	50.395	40.387	101.332	46.980
27	29.999	44.767	123.399	49.720
28	32.370	42.254	61.605	58.309
29	28.799	54.420	64.316	58.422
30	46.548	55.289	55.242	78.626
31	24.295	56.607	105.527	67.035
32	39.474	53.141	51.657	73.565
33	45.663	46.053	58.090	53.287
34	34.871	54.845	101.046	65.990
35	34.537	53.442	61.622	68.254
36	39.680	52.406	59.573	64.122
37	45.013	60.437	73.141	72.141
38	31.718	49.990	61.763	64.494

Table 4.2 Results obtained from the whole cell and the cell nucleus for HNF1A protein in siRNA-treated cells. (Continued)

39	49.622	49.522	82.284	82.925
40	36.220	48.994	116.171	70.393
41	41.582	59.142	111.669	74.003
42	47.164	44.028	70.591	88.264
43	37.222	33.956	77.486	83.549
44	39.834	38.804	64.626	67.823
45	37.733	47.576	108.004	55.476
46	36.083	49.415	95.168	65.749
47	44.816	36.102	115.217	67.269
48	49.938	44.243	107.865	63.280
49	50.743	47.142	108.237	81.524
50	46.615	37.416	120.987	71.686
51	47.742	28.827	106.957	65.617
52	48.701	34.760	91.395	74.055
53	40.336	69.786	77.220	78.929
54	34.683	58.147	80.491	78.573
55	22.914	49.594	48.049	71.654
56	30.596	44.881	75.667	84.177
Mean	**35.876**	**48.003**	**78.283**	**66.289**
Standard deviation	8.593	10.302	23.940	10.696
Min	20.800	28.792	35.538	45.638
Max	50.743	69.786	123.399	88.264

4.4.1.1 Effects of Kpna-specific siRNA on The Level of Kpna Protein in MIN6 Cells

Kpna-specific siRNA treatment is expected to decrease the level of Kpna protein in Min6 cells. Thus, Kpna protein level was analyzed in siRNA-treated and untreated cells as shown in Figure 4.8. Kpna6 transport protein was mostly localized in the cytoplasm. The Kpna6 signal obtained from the Kpna6-specific siRNA treated cells was found to be less when compared to the control negative non-treated and siRNA-treated cells.

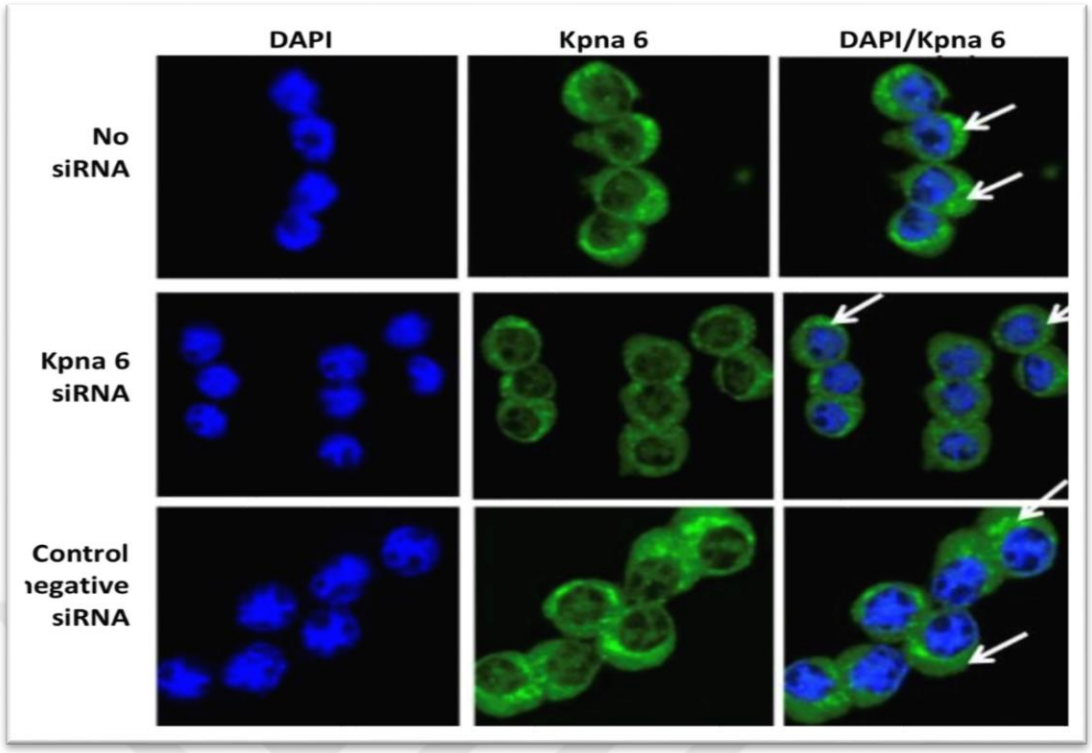


Figure 4.8 Analysis of nuclear localization of Kpna6 transport protein in Kpna6-specific siRNA-treated, negative control siRNA-treated and non-treated Min6 cells. DAPI was used to stain the cell nucleus.Kpna6 proteins were mostly localized in the cytoplasm as shown by the arrows.

Table 4.3 exhibits the Kpna6 protein levels from siRNA-treated and non-treated cells. Since the mean area of the cells obtained from both calculations was different from each other, the area and the mean values were adjusted according to the highest value to compare the levels. Therefore, approximately 23% reduction in Kpna6 level was achieved by siRNA application.

Table 4.3 Results obtained from the whole cell for Kpna6 protein in siRNA-treated and non-treated cells.

	siRNA Treated cells		**siRNA Non-treated cells**	
Cell No.	**Area (micron)**	**Average signal (pixels/micron)**	**Area (micron)**	**Average signal (pixels/micron)**
1	170.983	70.47	198.437	54.717
2	125.945	66.601	151.310	54.452
3	107.253	68.942	143.276	54.815
4	79.516	88.651	120.592	47.996
5	86.687	31.324	175.583	49.351

Table 4.3 Results obtained from the whole cell for Kpna6 protein in siRNA-treated and non-treated cells. (Continued)

6	178.538	27.889	117.923	42.404
7	127.934	25.073	80.195	39.564
8	117.277	31.797	89.833	51.104
9	275.075	31.841	58.713	49.933
10	182.499	30.746	97.704	53.883
11	138.34	35.887	138.949	49.323
12	129.718	40.307	52.749	56.441
13	139.747	38.136	47.378	51.621
14	151.921	59.019	57.800	54.021
15	85.195	56.893	45.592	53.122
16	77.446	53.555	73.293	60.815
17	58.79	55.609	76.392	62.383
18	67.624	60.802	63.919	63.951
19	56.159	68.286	65.647	60.958
20	78.523	63.761	74.391	54.057
21	61.074	61.085	54.609	54.211
22	54.581	63.031	61.510	50.968
23	63.563	62.753	143.883	56.446
24	57.517	64.168	64.860	49.719
25	58.412	61.709	62.900	51.203
26	132.543	48.576	135.012	58.920
27	75.575	56.167	85.774	56.176
28	64.038	55.413	84.731	65.050
29	61.612	55.633	60.488	61.459
30	113.768	53.108	50.762	49.723
31	112.338	49.213	64.174	60.929
32	130.041	52.754	55.054	54.486
33	171.235	57.028	55.124	67.762
34	73.746	71.862	69.697	65.248
35	64.967	66.317	58.032	60.465
36	110.605	61.716	67.858	75.996
37	110.094	63.875	48.646	65.632

Table 4.3 Results obtained from the whole cell for Kpna6 protein in siRNA-treated and non-treated cells. (Continued)

38	126.459	66.607	75.918	63.231
39	110.986	58.022	55.160	70.297
40	69.621	65.71	58.570	57.121
41	210.584	67.614	61.556	59.814
42	115.544	78.285	50.516	56.988
43	125.042	70.276	62.752	63.122
44	128.278	67.899	68.199	52.981
45	132.614	63.452	73.352	56.385
Mean	**107.719**	**57.862**	**81.307**	**56.650**
Fixed mean	**107.719**	**57.862**	**107.719**	**75.22**
Standard diviation	46.725	14.64	36.785	7.061
Min	54.581	25.073	45.592	39.564
Max	275.075	88.651	198.437	75.996

4.4.2 Effects of Control Negative siRNA Treatment on HNF1A and Kpna6 Protein Levels

In the siRNA study, “Silencer select negative siRNA, Thermo Fisher “was used as the control. The results obtained for HNF1A protein levels in this study are shown in Table 4.4. By comparing them with non-treated cells, it was found that approximately 80% of the HNF1A protein was localized in the cell nucleus and the negative siRNA did not cause any significant change.

Table 4.4 Results obtained from the whole cell and the cell nucleus in control negative siRNA-treated cells for HNF1A protein.

	Cell nucleus		**Whole cell**	
Cell No.	**Area (micron)**	**Average signal (pixels/micron)**	**Area (micron)**	**Average signal (pixels/micron)**
1	38.648	25.770	106.227	37.981
2	35.267	29.701	80.381	40.409
3	37.717	30.496	78.512	36.879
4	20.348	26.270	92.123	36.203
5	30.805	34.977	47.981	38.821

Table 4.4 Results obtained from the whole cell and the cell nucleus in control negative siRNA-treated cells for HNF1A protein. (Continued)

6	27.211	27.100	45.197	31.457
7	23.072	25.798	102.741	45.214
8	45.596	33.348	108.426	43.287
9	43.391	25.212	86.330	35.458
10	31.651	24.788	83.901	34.567
11	47.631	30.302	106.201	31.694
12	54.805	33.842	114.741	40.959
13	34.305	62.547	124.052	42.917
14	40.093	47.856	88.152	38.890
15	34.412	42.773	145.970	32.949
16	37.919	60.236	62.956	65.441
17	39.785	55.852	56.629	52.947
18	34.341	42.835	56.598	61.493
19	30.690	40.087	68.537	58.719
20	31.263	37.300	63.034	60.125
21	23.256	36.261	73.336	66.348
22	36.840	50.707	58.173	51.970
23	31.171	37.921	51.481	46.624
24	29.728	40.023	89.859	46.945
25	29.522	42.096	56.133	47.625
26	29.809	39.272	44.028	54.692
27	57.011	23.334	64.519	53.482
28	34.637	28.342	41.632	51.682
29	48.528	30.491	125.299	36.211
30	44.972	31.666	80.760	36.473
31	54.065	24.570	65.269	41.449
32	27.942	30.893	77.648	44.997
33	39.799	32.011	75.019	37.339
34	34.491	27.165	72.273	36.604
Mean	**36.492**	**35.642**	**79.239**	**44.672**
Standard deviation	8.981	10.264	25.736	9.855
Min	20.348	23.334	41.632	31.457
Max	57.011	62.547	145.970	66.348

Control siRNA showed no significant change in the amount of Kpna6 protein in the cell. Results for Kpna6 protein are shown in Table 4.5 as the cell areas were different from

each other when compared to the non-siRNA treated cells, the mean values were adjusted and compared accordingly.

Table 4.5 Results obtained from the whole cell in control negative siRNA-treated cells for Kpna6 protein.

	Whole cell	
Cell No.	**Area (micron)**	**Average signal (pixels/micron)**
1	134.556	40.306
2	74.124	45.688
3	73.321	49.534
4	97.144	45.544
5	41.849	34.184
6	61.773	45.397
7	105.712	43.237
8	84.049	44.051
9	118.739	49.988
10	85.094	44.128
11	65.940	77.730
12	49.915	65.393
13	62.496	72.667
14	57.421	71.531
15	68.037	68.863
16	76.136	79.074
17	58.891	64.309
18	55.171	65.439
19	60.851	56.681
20	55.081	60.301
21	45.941	66.079
22	63.097	66.615
23	43.711	64.755
24	73.473	57.445
25	61.401	55.842
26	79.952	46.345
27	72.502	50.627
28	73.745	49.131

Table 4.5 Results obtained from the whole cell in control negative siRNA-treated cells for Kpna6 protein. (Continued)

29	97.144	45.544
30	146.419	47.300
31	126.394	39.362
32	104.498	52.725
Mean	**77.330**	**55.182**
Fixed mean	**107.719**	**77.14**
Standard deviation	26.606	11.971
Min	41.849	34.184
Max	146.419	79.074

Results from the immunocytochemical staining analysis for HNF1A and Kpna6 proteins are shown in Figure 4.9 as a chart.

A)

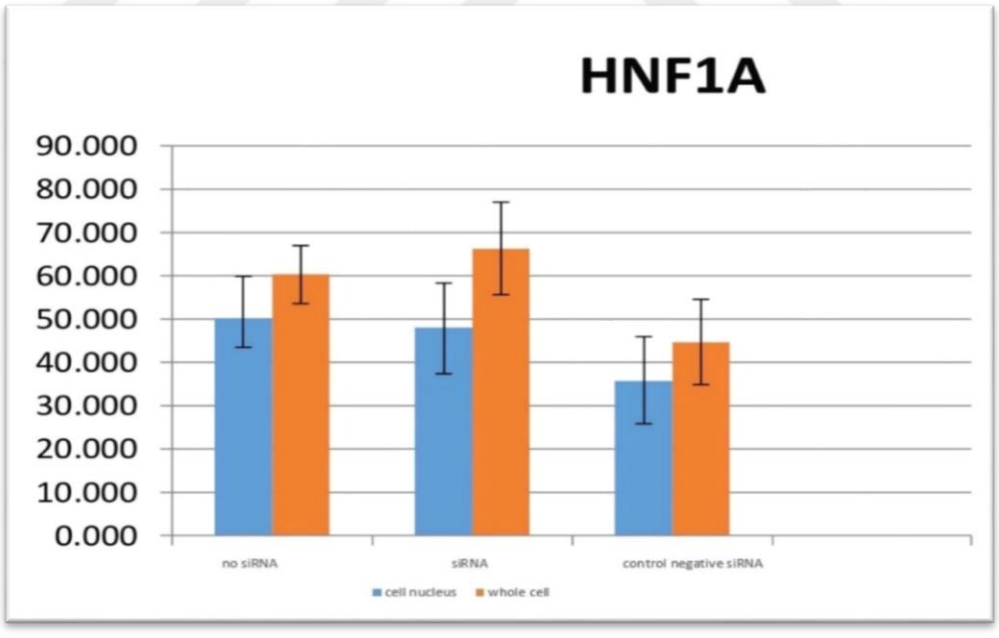


Figure 4.9. Results immunocytochemical staining and confocal analysis in siRNA treated cells, control negative siRNA-treated and non-treated cells for A) HNF1A and B) Kpna6 proteins.

B)

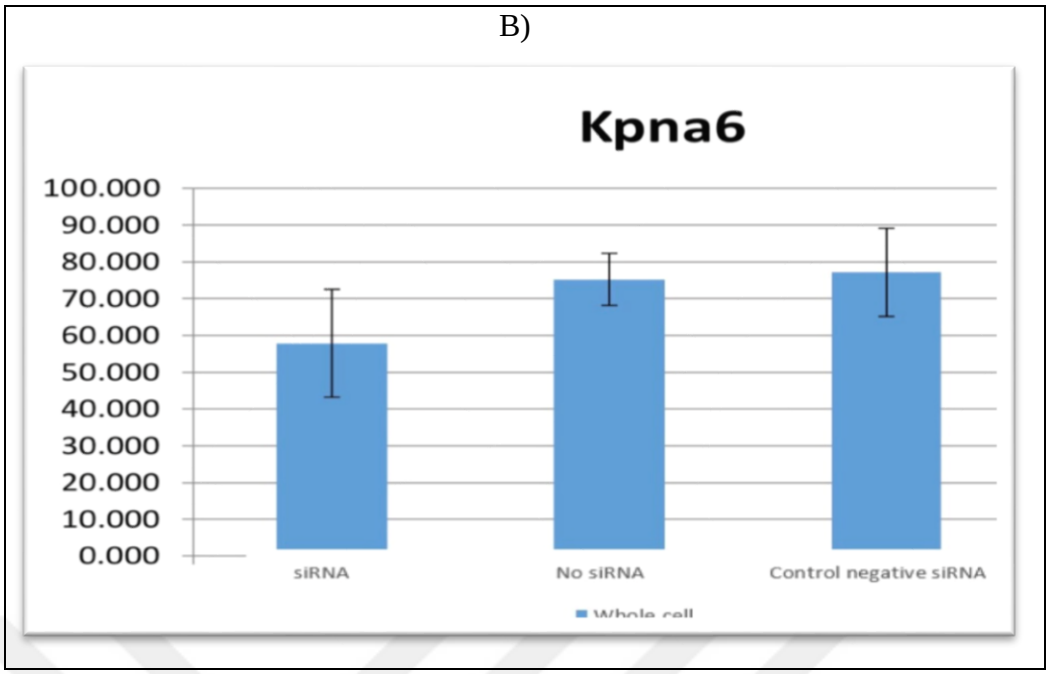


Figure 4.9. Results immunocytochemical staining and confocal analysis in siRNA treated cells, control negative siRNA-treated and non-treated cells for A) HNF1A and B) Kpna6 proteins. (Continued)

4.4.3 Analysis of Co-localization of HNF1A and Kpna6 Proteins by Using Immunocytochemical Staining

Immunocytochemical data also revealed that Kpna6 (green) and HNF1A (red) co-localized as overlapping domains of expression are observed as yellow in mostly cytoplasm of the Min6 cells are shown in Figure 4.10 these results also confirm the data obtained by the co-immunoprecipitation assay.

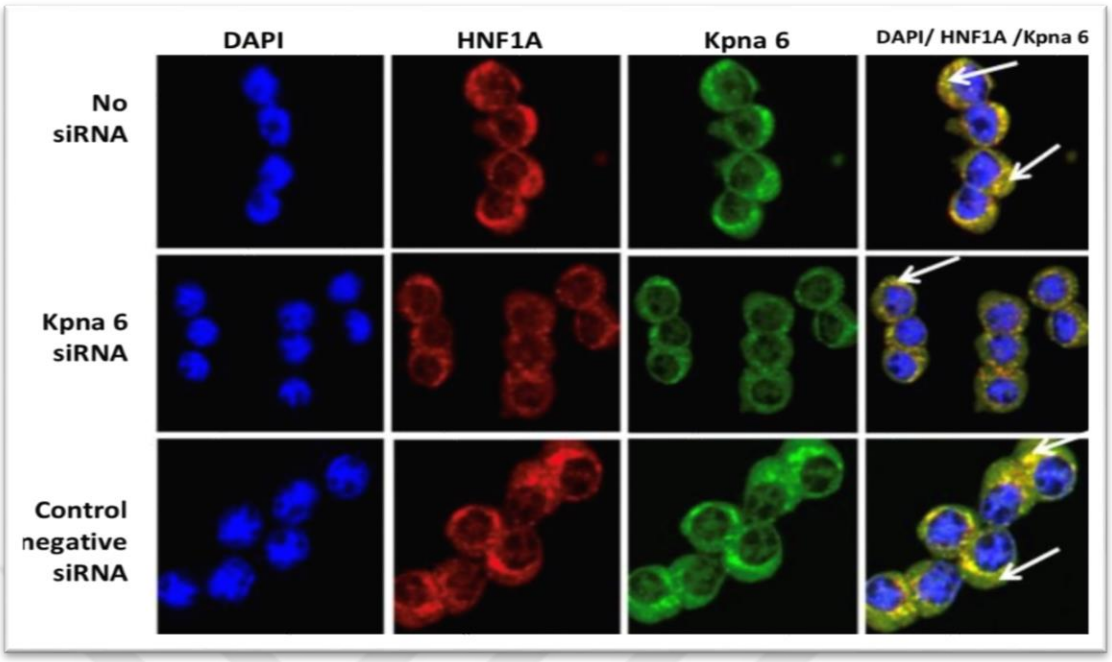


Figure 4.10. Co-localization of Kpna6 transport protein and HNF1A proteins in the cytoplasm of Min6 cells were shown by arrows. DAPI was used to stain the cell nucleus.

CHAPTER 5

RESULTS AND DISCUSSION

Functional characterization of HNF1A gene mutations identified in MODY3 patients revealed that they might affect DNA binding, transactivation function or nuclear localization of HNF1A. In previous studies, R171X, R271W, A276D, Q466X, and P379fsdelCT HNF1A mutant proteins exhibited impaired nuclear localization [139]. Also, A functional analysis was conducted for S345Y candidate mutation in the HNF1A gene found in a MODY suspected patient within the scope of a career development project (3501). In this study, the localization of S345Y mutant HNF1A protein to the cell nucleus was found to be defective as shown in Figure5.1 (unpublished data).

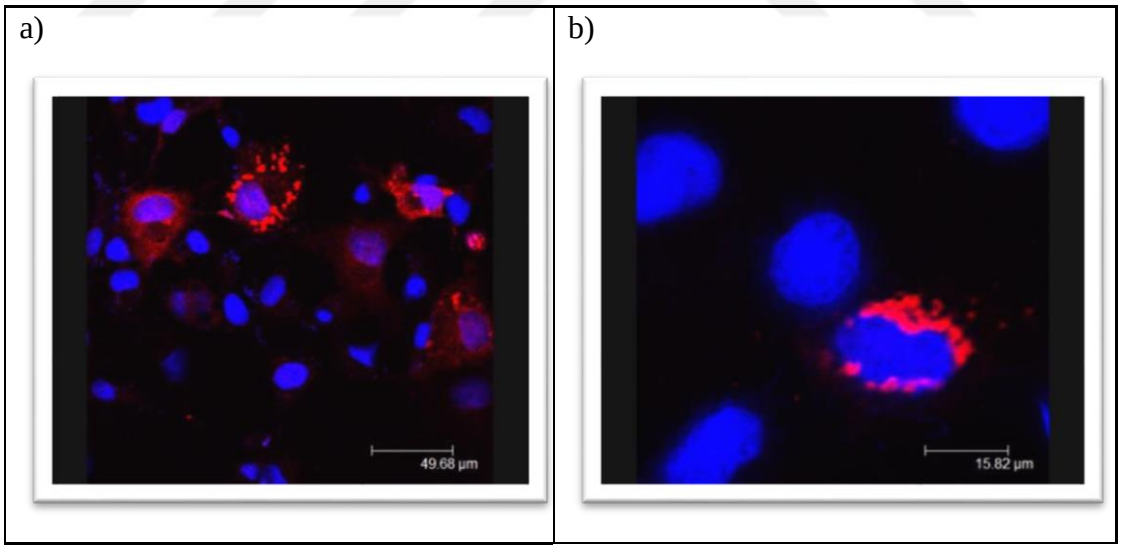


Figure 5.1. Impaired nuclear localization of S345Y mutation which resides in the non-classical NLS region. a) Wild-type b) S345Y mutant HNF1A transcription factor nuclear localization in COS-7 cells. The nucleus of cells was stained with blue color DAPI, wild/ mutant HNF1A were stained with red color.

These findings provided the starting point to clarify the import pathway of HNF1A protein and to find out which importin α protein subfamily is responsible for recognizing and translocating HNF1A protein to the cell nucleus [139]. Understanding

the import pathway will provide the pieces of evidence for the reason behind the cytoplasmic accumulation of the mutant HNF1A proteins (R271W and S345Y) [139]. To date, nuclear localization signals on HNF1A protein has not been studied in detail, but three regions fit the description of an NLS: region A (amino acids 158-171), region B (amino acids 197-205) and region C (amino acids 271-282). However, importin α subtype which recognizes and binds to HNF1A has not been reported yet. R217 is a positively charged amino acid which constructs the N-terminal cluster of nuclear localization signal in C region (271-288) of HNF1A.R271W mutation causes defective nuclear localization, and the protein was found be accumulated in the cytoplasm [139]. S345Y mutation, on the other hand, resides in a region which does not fit to the definition of classical nuclear localization signal. For this reason, this region is a new candidate for non-classical nuclear localization signals.

For this purpose, importin α1, α3, and α7 and amino acid sequences of human importin α subgroups have been studied with a very similar and conserved mouse homologs karyopherin α proteins (Kpna2, 4 and 6). Co-immunoprecipitation studies demonstrated surprisingly that all of the examined importin α proteins were able to bind to the nuclear localization signal of the wild-type HNF1A protein. To validate the results, this experiment was repeated at least 3 times and showed that the strongest band was with Kpna6 protein. It has also been decided that the study should proceed with this protein for the next stages because of the high level of expression of the Kpna6 protein in the pancreas.

The results obtained by the co-immunoprecipitation study were also validated by immunocytochemical staining as HNF1A and Kpna6 proteins co-localized in the cytoplasm. Kpna6- specific siRNA treatment showed 10% less localization of HNF1A to the nucleus. This implies that knockdown of Kpna6 protein does not make a significant difference, because the HNF1A protein is also recognized and bound by other carrier proteins (Kpna2 and 4). Furthermore, previous studies showed that when a specific importin α subgroup is knocked down and silenced in mouse models, the cargo proteins are transported by other subgroups *in vivo* [86]. With siRNA application, a 23% reduction in the level of Kpna6 protein in the whole cell was detected. Therefore if the level of Kpna6 protein can be reduced more, a higher amount of HNF1A protein can be localized in the cytoplasm. For this purpose, the amount of siRNA administered can be increased, but this can cause a cytotoxic effect and lead to cell death.

Another aim of the project was to investigate the interaction of the R271W and S345Y mutant proteins which were previously identified in MODY patients, with the transport protein Kpna6. The R271W mutation is located within the classical NLS region (C-region) of the basic amino acid of HNF1A [1]. Arginine (R) is a basic amino acid which was found to be essential for nuclear binding and tryptophan (W) is a polar amino acid with an aromatic group [1]. This basic amino acid alteration in the NLS region of the HNF1A protein reduced the binding ability significantly to the transport protein Kpna6. Although the S345Y mutation was located in a region which was not previously identified as a classical NLS, co-immunoprecipitation studies have shown that the alteration in this region also reduces recognition and binding ability to the Kpna6 protein. In a previous study, the interactions between the non-classical NLS of the influenza A virus nucleoprotein and the importin proteins were analyzed [140]. This study proved that classical-NLS and non-classical NLS bind to importin-α from different binding sites. Also, it showed that the ncNLS region is an essential factor in the molecular transportation, for any alteration in this region will decrease the binding ability to importin-α [140]. These findings will be the preliminary results for the future projects to understand further and analyze the non-classical NLS region.

REFERENCES

[1] Bjorkhaug, L. Bratland, A. Njolstad, P.R. Ve Molven, A., (2005). "Functional Dissection Of The HNF-1alpha Transcription Factor: A Study On Nuclear Localization And Transcriptional Activation", DNA Cell Biol, 24: 661-669.

[2] Tattersall, R.B. Ve Fajans, S.S., (1975). "A Difference Between The Inheritance Of Classical Juvenile-Onset And Maturity-Onset Type Diabetes Of Young People", Diabetes, 24: 44-53.

[3] Tattersall, R.B., (1974). "Mild Familial Diabetes With Dominant Inheritance", Q J Med, 43: 339-357.

[4] Bonnefond, A. Froguel, P. Ve Vaxillaire, M., (2010). "The Emerging Genetics Of Type 2 Diabetes", Trends Mol Med, 16: 407-416.

[5] Bowman, P. Flanagan, S.E. Edghill, E.L. Damhuis, A. Shepherd, M.H. Paisey, R. Hattersley, A.T. Ve Ellard, S., (2012). "Heterozygous ABCC8 Mutations Are A Cause Of MODY", Diabetologia, 55: 123-127.

[6] Fajans, S.S. Ve Bell, G.I., (2011). "MODY: History, Genetics, Pathophysiology, And Clinical Decision Making", Diabetes Care, 34: 1878-1884.

[7] Bonnefond, A. Philippe, J. Durand, E. Dechaume, A. Huyvaert, M. Montagne, L. Marre, M. Balkau, B. Fajardy, I. Vambergue, A. Vatin, V. Delplanque, J. Le Guilcher, D. De Graeve, F. Lecoeur, C. Sand, O. Vaxillaire, M. Ve Froguel, P., (2012). "Whole-Exome Sequencing And High Throughput Genotyping Identified KCNJ11 As The Thirteenth MODY Gene", Plos One, 7: E37423.

[8] Wang, H. Antinozzi, P.A. Hagenfeldt, K.A. Maechler, P. Ve Wollheim, C.B., (2000). "Molecular Targets Of A Human HNF1 Alpha Mutation Responsible For Pancreatic Beta-Cell Dysfunction", Embo J, 19: 4257-4264.

[9] Ellard, S. Ve Colclough, K., (2006). "Mutations In The Genes Encoding The Transcription Factors Hepatocyte Nuclear Factor 1 Alpha (HNF1A) And 4 Alpha (HNF4A) In Maturity-Onset Diabetes Of The Young", Hum Mutat, 27: 854-869.

[10] Kalderon, D. Richardson, W.D. Markham, A.F. Ve Smith, A.E., (1984). "Sequence Requirements For Nuclear Location Of Simian Virus 40 Large-T Antigen", Nature, 311: 33-38.

[11] Robbins, J. Dilworth, S.M. Laskey, R.A. Ve Dingwall, C., (1991). "Two Interdependent Basic Domains In Nucleoplasmin Nuclear Targeting Sequence: Identification Of A Class Of Bipartite Nuclear Targeting Sequence", Cell, 64: 615-623.

[12] Dingwall, C. Ve Laskey, R.A., (1991). "Nuclear Targeting Sequences--A Consensus?", Trends Biochem Sci, 16: 478-481.
[13] Gorlich, D. Ve Mattaj, I.W., (1996). "Nucleocytoplasmic Transport", Science, 271: 1513-1518.
[14] Goldfarb, D.S. Corbett, A.H. Mason, D.A. Harreman, M.T. Ve Adam, S.A., (2004). "Importin Alpha: A Multipurpose Nuclear-Transport Receptor", Trends Cell Biol, 14: 505-514.
[15] Hatayama, M. Tomizawa, T. Sakai-Kato, K. Bouvagnet, P. Kose, S. Imamoto, N. Yokoyama, S. Utsunomiya-Tate, N. Mikoshiba, K. Kigawa, T. Ve Aruga, J., (2008). "Functional And Structural Basis Of The Nuclear Localization Signal In The ZIC3 Zinc Finger Domain", Human Molecular Genetics, 17: 3459-3473.
[16] Hogarth, C.A. Calanni, S. Jans, D.A. Ve Loveland, K.L., (2006). "Importin Alpha Mrnas Have Distinct Expression Profiles During Spermatogenesis", Dev Dyn, 235: 253-262.
[17] Anik, A. Catli, G. Abaci, A. Ve Bober, E., (2015). "Maturity-Onset Diabetes Of The Young (MODY): An Update", J Pediatr Endocrinol Metab, 28: 251-263.
[18] Schwitzgebel, V.M., (2014). "Many Faces Of Monogenic Diabetes", J Diabetes Investig, 5: 121-133.
[19] Ashcroft, F.M. Ve Rorsman, P., (2012). "Diabetes Mellitus And The Beta Cell: The Last Ten Years", Cell, 148: 1160-1171.
[20] Prudente, S. Jungtrakoon, P. Marucci, A. Ludovico, O. Buranasupkajorn, P. Mazza, T. Hastings, T. Milano, T. Morini, E. Mercuri, L. Bailetti, D. Mendonca, C. Alberico, F. Basile, G. Romani, M. Miccinilli, E. Pizzuti, A. Carella, M. Barbetti, F. Pascarella, S. Marchetti, P. Trischitta, V. Di Paola, R. Ve Doria, A., (2015). "Loss-Of-Function Mutations In APPL1 In Familial Diabetes Mellitus", American Journal Of Human Genetics, 97: 177-185.
[21] Price, A.L. Patterson, N.J. Plenge, R.M. Weinblatt, M.E. Shadick, N.A. Ve Reich, D., (2006). "Principal Components Analysis Corrects For Stratification In Genome-Wide Association Studies", Nat Genet, 38: 904-909.
[22] Fajans, S.S. Bell, G.I. Ve Polonsky, K.S., (2001). "Molecular Mechanisms And Clinical Pathophysiology Of Maturity-Onset Diabetes Of The Young", N Engl J Med, 345: 971-980.
[23] Nyunt, O. Wu, J.Y. Mcgown, I.N. Harris, M. Huynh, T. Leong, G.M. Cowley, D.M. Ve Cotterill, A.M., (2009). "Investigating Maturity Onset Diabetes Of The Young", Clin Biochem Rev, 30: 67-74.
[24] Kim, S.H. Ma, X. Weremowicz, S. Ercolino, T. Powers, C. Mlynarski, W. Bashan, K.A. Warram, J.H. Mychaleckyj, J. Rich, S.S. Krolewski, A.S. Ve Doria, A., (2004). "Identification Of A Locus For Maturity-Onset Diabetes Of The Young On Chromosome 8p23", Diabetes, 53: 1375-1384.
[25] Reiner, T. Kohler, R.H. Liew, C.W. Hill, J.A. Gaglia, J. Kulkarni, R.N. Ve Weissleder, R., (2010). "Near-Infrared Fluorescent Probe For Imaging Of Pancreatic Beta Cells", Bioconjugate Chemistry, 21: 1362-1368.
[26] Raeder, H. Johansson, S. Holm, P.I. Haldorsen, I.S. Mas, E. Sbarra, V. Nermoen, I. Eide, S.A. Grevle, L. Bjorkhaug, L. Sagen, J.V. Aksnes, L. Sovik, O. Lombardo, D. Molven, A. Ve Njolstad, P.R., (2006). "Mutations In The CEL VNTR Cause A Syndrome Of Diabetes And Pancreatic Exocrine Dysfunction", Nat Genet, 38: 54-62.
[27] Johansson, B.B. Torsvik, J. Bjorkhaug, L. Vesterhus, M. Ragvin, A. Tjora, E. Fjeld, K. Hoem, D. Johansson, S. Raeder, H. Lindquist, S. Hernell, O. Cnop,

M. Saraste, J. Flatmark, T. Molven, A. Ve Njolstad, P.R., (2011). "Diabetes And Pancreatic Exocrine Dysfunction Due To Mutations In The Carboxyl Ester Lipase Gene-Maturity Onset Diabetes Of The Young (CEL-MODY): A Protein Misfolding Disease", J Biol Chem, 286: 34593-34605.

[28] Froguel, P. Zouali, H. Vionnet, N. Velho, G. Vaxillaire, M. Sun, F. Lesage, S. Stoffel, M. Takeda, J. Passa, P. Ve Et Al., (1993). "Familial Hyperglycemia Due To Mutations In Glucokinase. Definition Of A Subtype Of Diabetes Mellitus", N Engl J Med, 328: 697-702.

[29] Pearson, E.R. Velho, G. Clark, P. Stride, A. Shepherd, M. Frayling, T.M. Bulman, M.P. Ellard, S. Froguel, P. Ve Hattersley, A.T., (2001). "Beta-Cell Genes And Diabetes: Quantitative And Qualitative Differences In The Pathophysiology Of Hepatic Nuclear Factor-1alpha And Glucokinase Mutations", Diabetes, 50 Suppl 1: S101-107.

[30] Stride, A. Ellard, S. Clark, P. Shakespeare, L. Salzmann, M. Shepherd, M. Ve Hattersley, A.T., (2005). "Beta-Cell Dysfunction, Insulin Sensitivity, And Glycosuria Precede Diabetes In Hepatocyte Nuclear Factor-1alpha Mutation Carriers", Diabetes Care, 28: 1751-1756.

[31] Montoli, A. Colussi, G. Massa, O. Caccia, R. Rizzoni, G. Civati, G. Ve Barbetti, F., (2002). "Renal Cysts And Diabetes Syndrome Linked To Mutations Of The Hepatocyte Nuclear Factor-1 Beta Gene: Description Of A New Family With Associated Liver Involvement", Am J Kidney Dis, 40: 397-402.

[32] Bellanne-Chantelot, C. Chauveau, D. Gautier, J.F. Dubois-Laforgue, D. Clauin, S. Beaufils, S. Wilhelm, J.M. Boitard, C. Noel, L.H. Velho, G. Ve Timsit, J., (2004). "Clinical Spectrum Associated With Hepatocyte Nuclear Factor-1beta Mutations", Ann Intern Med, 140: 510-517.

[33] Ulinski, T. Lescure, S. Beaufils, S. Guigonis, V. Decramer, S. Morin, D. Clauin, S. Deschenes, G. Bouissou, F. Bensman, A. Ve Bellanne-Chantelot, C., (2006). "Renal Phenotypes Related To Hepatocyte Nuclear Factor-1beta (TCF2) Mutations In A Pediatric Cohort", J Am Soc Nephrol, 17: 497-503.

[34] Faguer, S. Decramer, S. Chassaing, N. Bellanne-Chantelot, C. Calvas, P. Beaufils, S. Bessenay, L. Lengele, J.P. Dahan, K. Ronco, P. Devuyst, O. Ve Chauveau, D., (2011). "Diagnosis, Management, And Prognosis Of HNF1B Nephropathy In Adulthood", Kidney Int, 80: 768-776.

[35] Pearson, E.R. Pruhova, S. Tack, C.J. Johansen, A. Castleden, H.A. Lumb, P.J. Wierzbicki, A.S. Clark, P.M. Lebl, J. Pedersen, O. Ellard, S. Hansen, T. Ve Hattersley, A.T., (2005). "Molecular Genetics And Phenotypic Characteristics Of MODY Caused By Hepatocyte Nuclear Factor 4alpha Mutations In A Large European Collection", Diabetologia, 48: 878-885.

[36] Shields, B.M. Hicks, S. Shepherd, M.H. Colclough, K. Hattersley, A.T. Ve Ellard, S., (2010). "Maturity-Onset Diabetes Of The Young (MODY): How Many Cases Are We Missing?", Diabetologia, 53: 2504-2508.

[37] Pearson, E.R. Boj, S.F. Steele, A.M. Barrett, T. Stals, K. Shield, J.P. Ellard, S. Ferrer, J. Ve Hattersley, A.T., (2007). "Macrosomia And Hyperinsulinaemic Hypoglycaemia In Patients With Heterozygous Mutations In The HNF4A Gene", Plos Med, 4: E118.

[38] Aydin, B.K. Bundak, R. Baş, F. Maraş, H. Saka, N. Günöz, H. Ve Darendeliler, F., (2012). "Permanent Neonatal Diabetes Mellitus: Same Mutation, Different Glycemic Control With Sulfonylurea Therapy On Long-

Term Follow-Up", Journal Of Clinical Research In Pediatric Endocrinology, 4: 107-110.

[39] Meur, G. Simon, A. Harun, N. Virally, M. Dechaume, A. Bonnefond, A. Fetita, S. Tarasov, A.I. Guillausseau, P.J. Boesgaard, T.W. Pedersen, O. Hansen, T. Polak, M. Gautier, J.F. Froguel, P. Rutter, G.A. Ve Vaxillaire, M., (2010). "Insulin Gene Mutations Resulting In Early-Onset Diabetes: Marked Differences In Clinical Presentation, Metabolic Status, And Pathogenic Effect Through Endoplasmic Reticulum Retention", Diabetes, 59: 653-661.

[40] Liu, L. Nagashima, K. Yasuda, T. Liu, Y. Hu, H.R. He, G. Feng, B. Zhao, M. Zhuang, L. Zheng, T. Friedman, T.C. Ve Xiang, K., (2013). "Mutations In KCNJ11 Are Associated With The Development Of Autosomal Dominant, Early-Onset Type 2 Diabetes", Diabetologia, 56: 2609-2618.

[41] Neve, B. Fernandez-Zapico, M.E. Ashkenazi-Katalan, V. Dina, C. Hamid, Y.H. Joly, E. Vaillant, E. Benmezroua, Y. Durand, E. Bakaher, N. Delannoy, V. Vaxillaire, M. Cook, T. Dallinga-Thie, G.M. Jansen, H. Charles, M.A. Clement, K. Galan, P. Hercberg, S. Helbecque, N. Charpentier, G. Prentki, M. Hansen, T. Pedersen, O. Urrutia, R. Melloul, D. Ve Froguel, P., (2005). "Role Of Transcription Factor KLF11 And Its Diabetes-Associated Gene Variants In Pancreatic Beta Cell Function", Proc Natl Acad Sci U S A, 102: 4807-4812.

[42] Fernandez-Zapico, M.E. Van Velkinburgh, J.C. Gutierrez-Aguilar, R. Neve, B. Froguel, P. Urrutia, R. Ve Stein, R., (2009). "MODY7 Gene, KLF11, Is A Novel P300-Dependent Regulator Of Pdx-1 (MODY4) Transcription In Pancreatic Islet Beta Cells", J Biol Chem, 284: 36482-36490.

[43] Malecki, M.T. Jhala, U.S. Antonellis, A. Fields, L. Doria, A. Orban, T. Saad, M. Warram, J.H. Montminy, M. Ve Krolewski, A.S., (1999). "Mutations In NEUROD1 Are Associated With The Development Of Type 2 Diabetes Mellitus", Nat Genet, 23: 323-328.

[44] Kristinsson, S.Y. Thorolfsdottir, E.T. Talseth, B. Steingrimsson, E. Thorsson, A.V. Helgason, T. Hreidarsson, A.B. Ve Arngrimsson, R., (2001). "MODY In Iceland Is Associated With Mutations In HNF-1alpha And A Novel Mutation In Neurod1", Diabetologia, 44: 2098-2103.

[45] Mauvais-Jarvis, F. Smith, S.B. Le May, C. Leal, S.M. Gautier, J.F. Molokhia, M. Riveline, J.P. Rajan, A.S. Kevorkian, J.P. Zhang, S. Vexiau, P. German, M.S. Ve Vaisse, C., (2004). "PAX4 Gene Variations Predispose To Ketosis-Prone Diabetes", Hum Mol Genet, 13: 3151-3159.

[46] Plengvidhya, N. Kooptiwut, S. Songtawee, N. Doi, A. Furuta, H. Nishi, M. Nanjo, K. Tantibhedhyangkul, W. Boonyasrisawat, W. Yenchitsomanus, P.T. Doria, A. Ve Banchuin, N., (2007). "PAX4 Mutations In Thais With Maturity Onset Diabetes Of The Young", J Clin Endocrinol Metab, 92: 2821-2826.

[47] Stoffers, D.A. Ferrer, J. Clarke, W.L. Ve Habener, J.F., (1997). "Early-Onset Type-II Diabetes Mellitus (MODY4) Linked To IPF1", Nat Genet, 17: 138-139.

[48] Odom, D.T. Zizlsperger, N. Gordon, D.B. Bell, G.W. Rinaldi, N.J. Murray, H.L. Volkert, T.L. Schreiber, J. Rolfe, P.A. Gifford, D.K. Fraenkel, E. Bell, G.I. Ve Young, R.A., (2004). "Control Of Pancreas And Liver Gene Expression By HNF Transcription Factors", Science, 303: 1378-1381.

[49] Colclough, K. Bellanne-Chantelot, C. Saint-Martin, C. Flanagan, S.E. Ve Ellard, S., (2013). "Mutations In The Genes Encoding The Transcription Factors Hepatocyte Nuclear Factor 1 Alpha And 4 Alpha In Maturity-Onset

Diabetes Of The Young And Hyperinsulinemic Hypoglycemia", Hum Mutat, 34: 669-685.

[50] Wollheim, C.B., (2000). "Beta-Cell Mitochondria In The Regulation Of Insulin Secretion: A New Culprit In Type II Diabetes", Diabetologia, 43: 265-277.

[51] Blumenfeld, M. Maury, M. Chouard, T. Yaniv, M. Ve Condamine, H., (1991). "Hepatic Nuclear Factor 1 (HNF1) Shows A Wider Distribution Than Products Of Its Known Target Genes In Developing Mouse", Development, 113: 589-599.

[52] Alves, C. Freitas, N. Ve Cunha, C., (2008). "Characterization Of The Nuclear Localization Signal Of The Hepatitis Delta Virus Antigen", Virology, 370: 12-21.

[53] Mendel, D.B. Ve Crabtree, G.R., (1991). "HNF-1, A Member Of A Novel Class Of Dimerizing Homeodomain Proteins", J Biol Chem, 266: 677-680.

[54] Kaisaki, P.J. Menzel, S. Lindner, T. Oda, N. Rjasanowski, I. Sahm, J. Meincke, G. Schulze, J. Schmechel, H. Petzold, C. Ledermann, H.M. Sachse, G. Boriraj, V.V. Menzel, R. Kerner, W. Turner, R.C. Yamagata, K. Ve Bell, G.I., (1997). "Mutations In The Hepatocyte Nuclear Factor-1alpha Gene In MODY And Early-Onset NIDDM: Evidence For A Mutational Hotspot In Exon 4", Diabetes, 46: 528-535.

[55] Glucksmann, M.A. Lehto, M. Tayber, O. Scotti, S. Berkemeier, L. Pulido, J.C. Wu, Y. Nir, W.J. Fang, L. Markel, P. Munnelly, K.D. Goranson, J. Orho, M. Young, B.M. Whitacre, J.L. Mcmenimen, C. Wantman, M. Tuomi, T. Warram, J. Forsblom, C.M. Carlsson, M. Rosenzweig, J. Kennedy, G. Duyk, G.M. Thomas, J.D. Ve Et Al., (1997). "Novel Mutations And A Mutational Hotspot In The MODY3 Gene", Diabetes, 46: 1081-1086.

[56] Gragnoli, C. Lindner, T. Cockburn, B.N. Kaisaki, P.J. Gragnoli, F. Marozzi, G. Ve Bell, G.I., (1997). "Maturity-Onset Diabetes Of The Young Due To A Mutation In The Hepatocyte Nuclear Factor-4 Alpha Binding Site In The Promoter Of The Hepatocyte Nuclear Factor-1 Alpha Gene", Diabetes, 46: 1648-1651.

[57] Vaxillaire, M. Rouard, M. Yamagata, K. Oda, N. Kaisaki, P.J. Boriraj, V.V. Chevre, J.C. Boccio, V. Cox, R.D. Lathrop, G.M. Dussoix, P. Philippe, J. Timsit, J. Charpentier, G. Velho, G. Bell, G.I. Ve Froguel, P., (1997). "Identification Of Nine Novel Mutations In The Hepatocyte Nuclear Factor 1 Alpha Gene Associated With Maturity-Onset Diabetes Of The Young (MODY3)", Hum Mol Genet, 6: 583-586.

[58] Cautain, B. Hill, R. De Pedro, N. Ve Link, W., (2015). "Components And Regulation Of Nuclear Transport Processes", Febs J, 282: 445-462.

[59] Kau, T.R. Way, J.C. Ve Silver, P.A., (2004). "Nuclear Transport And Cancer: From Mechanism To Intervention", Nat Rev Cancer, 4: 106-117.

[60] Stewart, M. Baker, R.P. Bayliss, R. Clayton, L. Grant, R.P. Littlewood, T. Ve Matsuura, Y., (2001). "Molecular Mechanism Of Translocation Through Nuclear Pore Complexes During Nuclear Protein Import", FEBS Lett, 498: 145-149.

[61] Tran, E.J. Ve Wente, S.R., (2006). "Dynamic Nuclear Pore Complexes: Life On The Edge", Cell, 125: 1041-1053.

[62] Rout, M.P. Aitchison, J.D. Suprapto, A. Hjertaas, K. Zhao, Y. Ve Chait, B.T., (2000). "The Yeast Nuclear Pore Complex: Composition, Architecture, And Transport Mechanism", J Cell Biol, 148: 635-651.

[63] Fahrenkrog, B. Maco, B. Fager, A.M. Koser, J. Sauder, U. Ullman, K.S. Ve Aebi, U., (2002). "Domain-Specific Antibodies Reveal Multiple-Site Topology Of Nup153 Within The Nuclear Pore Complex", J Struct Biol, 140: 254-267.
[64] Rout, M.P. Ve Wente, S.R., (1994). "Pores For Thought: Nuclear Pore Complex Proteins", Trends Cell Biol, 4: 357-365.
[65] Cronshaw, J.M. Krutchinsky, A.N. Zhang, W. Chait, B.T. Ve Matunis, M.J., (2002). "Proteomic Analysis Of The Mammalian Nuclear Pore Complex", J Cell Biol, 158: 915-927.
[66] Grote, M. Kubitscheck, U. Reichelt, R. Ve Peters, R., (1995). "Mapping Of Nucleoporins To The Center Of The Nuclear Pore Complex By Post-Embedding Immunogold Electron Microscopy", Journal Of Cell Science, 108: 2963.
[67] L. Paine, P. C. Moore, L. Ve B. Horowitz, S., (1975). Nuclear Envelope Permeability. Nature 254: 109-114.
[68] Newmeyer, D.D. Ve Forbes, D.J., (1988). "Nuclear Import Can Be Separated Into Distinct Steps In Vitro: Nuclear Pore Binding And Translocation", Cell, 52: 641-653.
[69] Radu, A. Blobel, G. Ve Moore, M.S., (1995). "Identification Of A Protein Complex That Is Required For Nuclear Protein Import And Mediates Docking Of Import Substrate To Distinct Nucleoporins", Proc Natl Acad Sci U S A, 92: 1769-1773.
[70] Gorlich, D. Prehn, S. Laskey, R.A. Ve Hartmann, E., (1994). "Isolation Of A Protein That Is Essential For The First Step Of Nuclear Protein Import", Cell, 79: 767-778.
[71] Stade, K. Ford, C.S. Guthrie, C. Ve Weis, K., (1997). "Exportin 1 (Crm1p) Is An Essential Nuclear Export Factor", Cell, 90: 1041-1050.
[72] Yoshida, K. Ve Blobel, G., (2001). "The Karyopherin Kap142p/Msn5p Mediates Nuclear Import And Nuclear Export Of Different Cargo Proteins", The Journal Of Cell Biology, 152: 729-740.
[73] Mahanty, S.K. Wang, Y. Farley, F.W. Ve Elion, E.A., (1999). "Nuclear Shuttling Of Yeast Scaffold Ste5 Is Required For Its Recruitment To The Plasma Membrane And Activation Of The Mating MAPK Cascade", Cell, 98: 501-512.
[74] Riddick, G. Ve Macara, I.G., (2005). "A Systems Analysis Of Importin-{Alpha}-{Beta} Mediated Nuclear Protein Import", The Journal Of Cell Biology, 168: 1027-1038.
[75] Ribbeck, K. Ve Görlich, D., (2001). "Kinetic Analysis Of Translocation Through Nuclear Pore Complexes", Embo J, 20: 1320-1330.
[76] Chook, Y.M. Ve Blobel, G., (2001). "Karyopherins And Nuclear Import", Curr Opin Struct Biol, 11: 703-715.
[77] Macara, I.G., (2001). "Transport Into And Out Of The Nucleus", Microbiology And Molecular Biology Reviews, 65: 570.
[78] Gorlich, D. Ve Kutay, U., (1999). "Transport Between The Cell Nucleus And The Cytoplasm", Annu Rev Cell Dev Biol, 15: 607-660.
[79] Conti, E. Ve Izaurralde, E., (2001). "Nucleocytoplasmic Transport Enters The Atomic Age", Curr Opin Cell Biol, 13: 310-319.
[80] Fahrenkrog, B. Ve Aebi, U., (2003). "The Nuclear Pore Complex: Nucleocytoplasmic Transport And Beyond", Nat Rev Mol Cell Biol, 4: 757-766.
[81] Mosammaparast, N. Ve Pemberton, L.F., (2004). "Karyopherins: From Nuclear-Transport Mediators To Nuclear-Function Regulators", Trends Cell Biol, 14: 547-556.

[82] Pemberton, L.F. Ve Paschal, B.M., (2005). "Mechanisms Of Receptor-Mediated Nuclear Import And Nuclear Export", Traffic, 6: 187-198.
[83] Madrid, A.S. Ve Weis, K., (2006). "Nuclear Transport Is Becoming Crystal Clear", Chromosoma, 115: 98-109.
[84] Conti, E. Muller, C.W. Ve Stewart, M., (2006). "Karyopherin Flexibility In Nucleocytoplasmic Transport", Curr Opin Struct Biol, 16: 237-244.
[85] Weis, K., (2003). "Regulating Access To The Genome: Nucleocytoplasmic Transport Throughout The Cell Cycle", Cell, 112: 441-451.
[86] Stewart, M., (2007). "Molecular Mechanism Of The Nuclear Protein Import Cycle", Nat Rev Mol Cell Biol, 8: 195-208.
[87] Smith, A. Brownawell, A. Ve Macara, I.G., (1998). "Nuclear Import Of Ran Is Mediated By The Transport Factor NTF2", Current Biology : CB, 8: 1403-1406.
[88] Conti, E. Uy, M. Leighton, L. Blobel, G. Ve Kuriyan, J., (1998). "Crystallographic Analysis Of The Recognition Of A Nuclear Localization Signal By The Nuclear Import Factor Karyopherin Alpha", Cell, 94: 193-204.
[89] Kim, Y.H. Han, M.E. Ve Oh, S.O., (2017). "The Molecular Mechanism For Nuclear Transport And Its Application", Anat Cell Biol, 50: 77-85.
[90] Kohler, A. Ve Hurt, E., (2007). "Exporting RNA From The Nucleus To The Cytoplasm", Nat Rev Mol Cell Biol, 8: 761-773.
[91] Chook, Y.M. Ve Suel, K.E., (2011). "Nuclear Import By Karyopherin-Betas: Recognition And Inhibition", Biochim Biophys Acta, 1813: 1593-1606.
[92] Hing, Z.A. Fung, H.Y. Ranganathan, P. Mitchell, S. El-Gamal, D. Woyach, J.A. Williams, K. Goettl, V.M. Smith, J. Yu, X. Meng, X. Sun, Q. Cagatay, T. Lehman, A.M. Lucas, D.M. Baloglu, E. Shacham, S. Kauffman, M.G. Byrd, J.C. Chook, Y.M. Garzon, R. Ve Lapalombella, R., (2016). "Next-Generation XPO1 Inhibitor Shows Improved Efficacy And In Vivo Tolerability In Hematological Malignancies", Leukemia, 30: 2364-2372.
[93] Huber, F.M. Ve Hoelz, A., (2017). "Molecular Basis For Protection Of Ribosomal Protein L4 From Cellular Degradation", Nature Communications, 8: 14354.
[94] Rose, A.S. Bradley, A.R. Valasatava, Y. Duarte, J.M. Prli, A. #263 Ve Rose, P.W., (2016). Web-Based Molecular Graphics For Large Complexes, Ed^Eds. Proceedings Of The 21st International Conference On Web3D Technology. Anaheim, California: ACM, 185-186.
[95] Rose, A.S. Ve Hildebrand, P.W., (2015). "NGL Viewer: A Web Application For Molecular Visualization", Nucleic Acids Research, 43: W576-W579.
[96] Pumroy, R.A. Ve Cingolani, G., (2015). "Diversification Of Importin-A Isoforms In Cellular Trafficking And Disease States", The Biochemical Journal, 466: 13-28.
[97] Conti, E. Ve Kuriyan, J., (2000). "Crystallographic Analysis Of The Specific Yet Versatile Recognition Of Distinct Nuclear Localization Signals By Karyopherin Alpha", Structure, 8: 329-338.
[98] Isoyama, T. Murayama, A. Nomoto, A. Ve Kuge, S., (2001). "Nuclear Import Of The Yeast AP-1-Like Transcription Factor Yap1p Is Mediated By Transport Receptor Pse1p, And This Import Step Is Not Affected By Oxidative Stress", J Biol Chem, 276: 21863-21869.
[99] Kaffman, A. Rank, N.M. Ve O'Shea, E.K., (1998). "Phosphorylation Regulates Association Of The Transcription Factor Pho4 With Its Import Receptor Pse1/Kap121", Genes Dev, 12: 2673-2683.

[100] Weis, K. Mattaj, I.W. Ve Lamond, A.I., (1995). "Identification Of Hsrp1 Alpha As A Functional Receptor For Nuclear Localization Sequences", Science, 268: 1049-1053.
[101] Cuomo, C.A. Kirch, S.A. Gyuris, J. Brent, R. Ve Oettinger, M.A., (1994). "Rch1, A Protein That Specifically Interacts With The RAG-1 Recombination-Activating Protein", Proc Natl Acad Sci U S A, 91: 6156-6160.
[102] Seki, T. Tada, S. Katada, T. Ve Enomoto, T., (1997). "Cloning Of A Cdna Encoding A Novel Importin-Alpha Homologue, Qip1: Discrimination Of Qip1 And Rch1 From Hsrp1 By Their Ability To Interact With DNA Helicase Q1/Recql", Biochem Biophys Res Commun, 234: 48-53.
[103] Wang, P. Palese, P. Ve O'Neill, R.E., (1997). "The NPI-1/NPI-3 (Karyopherin Alpha) Binding Site On The Influenza A Virus Nucleoprotein NP Is A Nonconventional Nuclear Localization Signal", J Virol, 71: 1850-1856.
[104] Nachury, M.V. Ryder, U.W. Lamond, A.I. Ve Weis, K., (1998). "Cloning And Characterization Of Hsrp1 Gamma, A Tissue-Specific Nuclear Transport Factor", Proc Natl Acad Sci U S A, 95: 582-587.
[105] Ushijima, R. Sakaguchi, N. Kano, A. Maruyama, A. Miyamoto, Y. Sekimoto, T. Yoneda, Y. Ogino, K. Ve Tachibana, T., (2005). "Extracellular Signal-Dependent Nuclear Import Of STAT3 Is Mediated By Various Importin Alphas", Biochem Biophys Res Commun, 330: 880-886.
[106] O'Neill, R.E. Ve Palese, P., (1995). "NPI-1, The Human Homolog Of SRP-1, Interacts With Influenza Virus Nucleoprotein", Virology, 206: 116-125.
[107] Cortes, P. Ye, Z.S. Ve Baltimore, D., (1994). "RAG-1 Interacts With The Repeated Amino Acid Motif Of The Human Homologue Of The Yeast Protein SRP1", Proc Natl Acad Sci U S A, 91: 7633-7637.
[108] Tachibana, T. Hieda, M. Miyamoto, Y. Kose, S. Imamoto, N. Ve Yoneda, Y., (2000). "Recycling Of Importin Alpha From The Nucleus Is Suppressed By Loss Of RCC1 Function In Living Mammalian Cells", Cell Struct Funct, 25: 115-123.
[109] Pettersen, E.F. Goddard, T.D. Huang, C.C. Couch, G.S. Greenblatt, D.M. Meng, E.C. Ve Ferrin, T.E., (2004). "UCSF Chimera--A Visualization System For Exploratory Research And Analysis", J Comput Chem, 25: 1605-1612.
[110] Fontes, M.R. Teh, T. Ve Kobe, B., (2000). "Structural Basis Of Recognition Of Monopartite And Bipartite Nuclear Localization Sequences By Mammalian Importin-Alpha", J Mol Biol, 297: 1183-1194.
[111] Hodel, M.R. Corbett, A.H. Ve Hodel, A.E., (2001). "Dissection Of A Nuclear Localization Signal", J Biol Chem, 276: 1317-1325.
[112] Hodel, A.E. Harreman, M.T. Pulliam, K.F. Harben, M.E. Holmes, J.S. Hodel, M.R. Berland, K.M. Ve Corbett, A.H., (2006). "Nuclear Localization Signal Receptor Affinity Correlates With In Vivo Localization In Saccharomyces Cerevisiae", J Biol Chem, 281: 23545-23556.
[113] Gilchrist, D. Ve Rexach, M., (2003). "Molecular Basis For The Rapid Dissociation Of Nuclear Localization Signals From Karyopherin Alpha In The Nucleoplasm", J Biol Chem, 278: 51937-51949.
[114] Timney, B.L. Tetenbaum-Novatt, J. Agate, D.S. Williams, R. Zhang, W. Chait, B.T. Ve Rout, M.P., (2006). "Simple Kinetic Relationships And Nonspecific Competition Govern Nuclear Import Rates In Vivo", J Cell Biol, 175: 579-593.
[115] Richardson, W.D. Roberts, B.L. Ve Smith, A.E., (1986). "Nuclear Location Signals In Polyoma Virus Large-T", Cell, 44: 77-85.

[116] Shaulsky, G. Goldfinger, N. Ben-Ze'ev, A. Ve Rotter, V., (1990). "Nuclear Accumulation Of P53 Protein Is Mediated By Several Nuclear Localization Signals And Plays A Role In Tumorigenesis", Mol Cell Biol, 10: 6565-6577.
[117] Henkel, T. Zabel, U. Van Zee, K. Muller, J.M. Fanning, E. Ve Baeuerle, P.A., (1992). "Intramolecular Masking Of The Nuclear Location Signal And Dimerization Domain In The Precursor For The P50 NF-Kappa B Subunit", Cell, 68: 1121-1133.
[118] Zabel, U. Henkel, T. Silva, M.S. Ve Baeuerle, P.A., (1993). "Nuclear Uptake Control Of NF-Kappa B By MAD-3, An I Kappa B Protein Present In The Nucleus", Embo J, 12: 201-211.
[119] Dingwall, C. Robbins, J. Dilworth, S.M. Roberts, B. Ve Richardson, W.D., (1988). "The Nucleoplasmin Nuclear Location Sequence Is Larger And More Complex Than That Of SV-40 Large T Antigen", The Journal Of Cell Biology, 107: 841-849.
[120] Dang, C.V. Ve Lee, W.M., (1988). "Identification Of The Human C-Myc Protein Nuclear Translocation Signal", Mol Cell Biol, 8: 4048-4054.
[121] Picard, D. Ve Yamamoto, K.R., (1987). "Two Signals Mediate Hormone-Dependent Nuclear Localization Of The Glucocorticoid Receptor", Embo J, 6: 3333-3340.
[122] Nemergut, M.E. Ve Macara, I.G., (2000). "Nuclear Import Of The Ran Exchange Factor, RCC1, Is Mediated By At Least Two Distinct Mechanisms", The Journal Of Cell Biology, 149: 835-850.
[123] Palmeri, D. Ve Malim, M.H., (1999). "Importin Beta Can Mediate The Nuclear Import Of An Arginine-Rich Nuclear Localization Signal In The Absence Of Importin Alpha", Mol Cell Biol, 19: 1218-1225.
[124] Truant, R. Ve Cullen, B.R., (1999). "The Arginine-Rich Domains Present In Human Immunodeficiency Virus Type 1 Tat And Rev Function As Direct Importin Beta-Dependent Nuclear Localization Signals", Mol Cell Biol, 19: 1210-1217.
[125] Hall, M.N. Hereford, L. Ve Herskowitz, I., (1984). "Targeting Of E. Coli Beta-Galactosidase To The Nucleus In Yeast", Cell, 36: 1057-1065.
[126] Yeh, C.T. Liaw, Y.F. Ve Ou, J.H., (1990). "The Arginine-Rich Domain Of Hepatitis B Virus Precore And Core Proteins Contains A Signal For Nuclear Transport", J Virol, 64: 6141-6147.
[127] Jakel, S. Ve Gorlich, D., (1998). "Importin Beta, Transportin, Ranbp5 And Ranbp7 Mediate Nuclear Import Of Ribosomal Proteins In Mammalian Cells", Embo J, 17: 4491-4502.
[128] Siomi, H. Ve Dreyfuss, G., (1995). "A Nuclear Localization Domain In The Hnrnp A1 Protein", J Cell Biol, 129: 551-560.
[129] Nagoshi, E. Ve Yoneda, Y., (2001). "Dimerization Of Sterol Regulatory Element-Binding Protein 2 Via The Helix-Loop-Helix-Leucine Zipper Domain Is A Prerequisite For Its Nuclear Localization Mediated By Importin Beta", Mol Cell Biol, 21: 2779-2789.
[130] Fanara, P. Hodel, M.R. Corbett, A.H. Ve Hodel, A.E., (2000). "Quantitative Analysis Of Nuclear Localization Signal (NLS)-Importin Alpha Interaction Through Fluorescence Depolarization. Evidence For Auto-Inhibitory Regulation Of NLS Binding", J Biol Chem, 275: 21218-21223.
[131] Harreman, M.T. Cohen, P.E. Hodel, M.R. Truscott, G.J. Corbett, A.H. Ve Hodel, A.E., (2003). "Characterization Of The Auto-Inhibitory Sequence

Within The N-Terminal Domain Of Importin Alpha", J Biol Chem, 278: 21361-21369.
[132] Gorlich, D. Kostka, S. Kraft, R. Dingwall, C. Laskey, R.A. Hartmann, E. Ve Prehn, S., (1995). "Two Different Subunits Of Importin Cooperate To Recognize Nuclear Localization Signals And Bind Them To The Nuclear Envelope", Current Biology : CB, 5: 383-392.
[133] Kobe, B. Jennings, I.G. House, C.M. Michell, B.J. Goodwill, K.E. Santarsiero, B.D. Stevens, R.C. Cotton, R.G. Ve Kemp, B.E., (1999). "Structural Basis Of Autoregulation Of Phenylalanine Hydroxylase", Nat Struct Biol, 6: 442-448.
[134] Fontes, M. Teh, T. Toth, G. John, A. Pavo, I. Jans, D. Ve Kobe, B., (2003). Role Of Flanking Sequences And Phosphorylation In The Recognition Of The Simian-Virus-40 Large T-Antigen Nuclear Localization Sequences By Importin-A.
[135] Neumann, G. Castrucci, M.R. Ve Kawaoka, Y., (1997). "Nuclear Import And Export Of Influenza Virus Nucleoprotein", J Virol, 71: 9690-9700.
[136] Cros, J.F. Garcia-Sastre, A. Ve Palese, P., (2005). "An Unconventional NLS Is Critical For The Nuclear Import Of The Influenza A Virus Nucleoprotein And Ribonucleoprotein", Traffic, 6: 205-213.
[137] Ye, Q. Krug, R.M. Ve Tao, Y.J., (2006). "The Mechanism By Which Influenza A Virus Nucleoprotein Forms Oligomers And Binds RNA", Nature, 444: 1078-1082.
[138] Ng, A.K. Zhang, H. Tan, K. Li, Z. Liu, J.H. Chan, P.K. Li, S.M. Chan, W.Y. Au, S.W. Joachimiak, A. Walz, T. Wang, J.H. Ve Shaw, P.C., (2008). "Structure Of The Influenza Virus A H5N1 Nucleoprotein: Implications For RNA Binding, Oligomerization, And Vaccine Design", Faseb J, 22: 3638-3647.
[139] Bjorkhaug, L. Sagen, J.V. Thorsby, P. Sovik, O. Molven, A. Ve Njolstad, P.R., (2003). "Hepatocyte Nuclear Factor-1 Alpha Gene Mutations And Diabetes In Norway", J Clin Endocrinol Metab, 88: 920-931.
[140] Nakada, R. Hirano, H. Ve Matsuura, Y., (2015). "Structure Of Importin-A Bound To A Non-Classical Nuclear Localization Signal Of The Influenza A Virus Nucleoprotein", Scientific Reports, 5: 15055-15055.

CURRICULUM VITAE

PERSONAL INFORMATION

Name Surname : Fareed Mohammed Ali Fareed FAREED
Date of Birth and Place : 26.1.1993
Foreign Languages : Arabic, English and Turkish
E-mail : fasaad32@gmail.com

EDUCATION

Degree	Department	University	Date of Graduation
Undergraduate	Chemistry	Al-mustansiriya University Collage	6 /2014
High School	General	Alandalos High School	6/2009

WORK EXPERIENCE

Year	Corporation/Institute	Enrollment
2014	Jannat Al-Harthea for Hormones and Clinical Blood Analysis (Baghdad ،Iraq)	2014-2015
2013	Department of Chemistry, College of Science, Al-Mustansyria University, Iraq	2013-2014

PUBLISHMENTS

Papers

1. Alkazaz. F.F., Abdulsattar, S.A., Fareed, F.M.A. and Mahmood, S. (2014). “Risk Factor Of Metabolism Alteration In Burn Patients”, Canadian Journal Of Pure And Applied Science, 8 (3-10): 3057-3060.

Conference Papers

1. Fareed, F.M.A., Korulu Koç, Ş., Sürme, S., Nalbantoğlu, B. and Yalçın Çapan, Ö. (2018). **“**Identification Of The Importin-Alpha Sub-Type That Is Responsible For The Import Of HNF1A Transcription Factor Into The Nucleus And The Analysis Of The Nuclear Localization Signal (NLS)”, 6th International Congress Of The Molecular Biology Association Of Turkey, 5-8 September 2018, Izmir.